CHEMISTRY OF MATERIALS

pubs.acs.org/cm

Review

Tools and Tricks for Single Crystal Growth

Tanya Berry,* Nicholas Ng,* and Tyrel M. McQueen*

Cite This: *Chem. Mater.* 2024, 36, 4929−4944

Read Online

ACCESS | Metrics & More | Article Recommendations

ABSTRACT: Single-crystal growth is a widely explored method of synthesizing materials in the solid state. The last few decades have seen significant improvements in the techniques used to synthesize single crystals, and much of this information has been collected and distributed via different papers and textbooks for the novice. What is often missing from these resources are perspectives on how to use these techniques in unusual ways, frequently combining aspects from different fields of chemistry. These variations on known single crystal growth techniques can help effect success in situations where the conventional technique might otherwise fail, as well as providing control over crucial structural defects. This manuscript informs about key aspects of single crystal growth techniques and variations that enable access to new materials and control over defects. We provide examples of materials that have been successfully grown as single crystals with each individual technique and highlight how the target material influences and informs the choice of technique and/or application of variations. Finally, we offer a case study, focusing on the floating zone technique, in which we delve into the growth of large single crystalline materials, as well as how the process can be influenced by modifications to attempt the growth of materials that might not otherwise be suitable for the technique. The presence of all of these sections in a single paper is meant to assist novice crystal growers in comparing, contrasting, and ultimately selecting a suitable technique or techniques for their experiments.

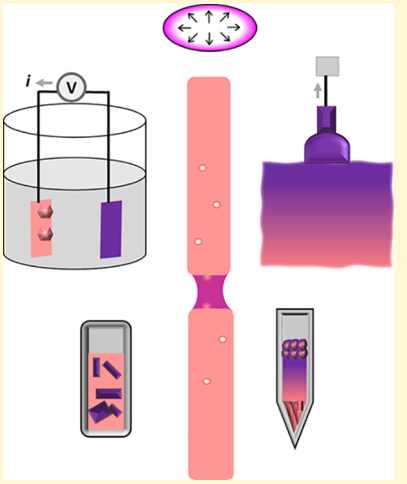

Downloaded via CORNELL UNIV on June 4, 2025 at 18:09:37 (UTC).
See https://pubs.acs.org/sharingguidelines for options on how to legitimately share published articles.

1. INTRODUCTION

Single crystals are crucial to materials discovery. The accurate determination of useful properties such as superconductivity and quantum magnetism often requires the use of single crystals, either in place of or in conjunction with polycrystalline or powder samples. Single crystals may exhibit physical properties that are different from their polycrystalline or amorphous counterparts and enable measurement and use of anisotropic, i.e., crystal direction-dependent, properties. These points can be critically important to the manufacturing of new materials with potential commercial use.

The thermodynamics and processes by which crystal growth occurs, from initial nucleation to bulk growth, as shown in Figure 1a, have been studied for many years and are in many respects well understood.[1−16] However, it is still not readily possible to grow single crystals of most materials. This dichotomy implies that we do not understand the processes well enough to know how the factors that are within our control, namely, the controllable growth parameters in methods available to us, influence and drive the microscopic thermodynamics and kinetics that fuel single crystal growth.

For the purposes of this Review, we will treat nucleation and growth as occurring at the interface between a fluid (liquid or gas) and a nascent solid, Figure 1b. From a chemical perspective, the challenges in predicting and designing crystal growths arise from the fact that there are a multitude of individual elementary steps occurring at the fluid−solid interface involving many bond-making and bond-breaking transformations and that these steps are highly dynamic in nature.[17] It is further complicated by the presence of molecular fragments in the fluid phase due to differential bond strengths between different pairs of elements, which alter the most relevant elementary steps and kinetically trap intermediate structures that would not be expected purely on thermodynamic grounds. As a result, predicting crystal growth is solved in the same sense that quantum mechanics has solved our understanding of the behavior of the Universe—which is to say while it may be solved in a mathematical sense of the governing equations having all been worked out, it is not practicable to generate meaningful predictions in most cases, and as a result, generating the requisite intuition and simplifying approaches remains a key challenge.

This challenge of nonpredictability has practical implications—including being the driving factor behind the large time gap between the discovery of a material and the ability to easily

Received: December 4, 2023
Revised: May 2, 2024
Accepted: May 7, 2024
Published: May 16, 2024

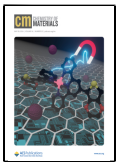

ACS Publications

© 2024 American Chemical Society

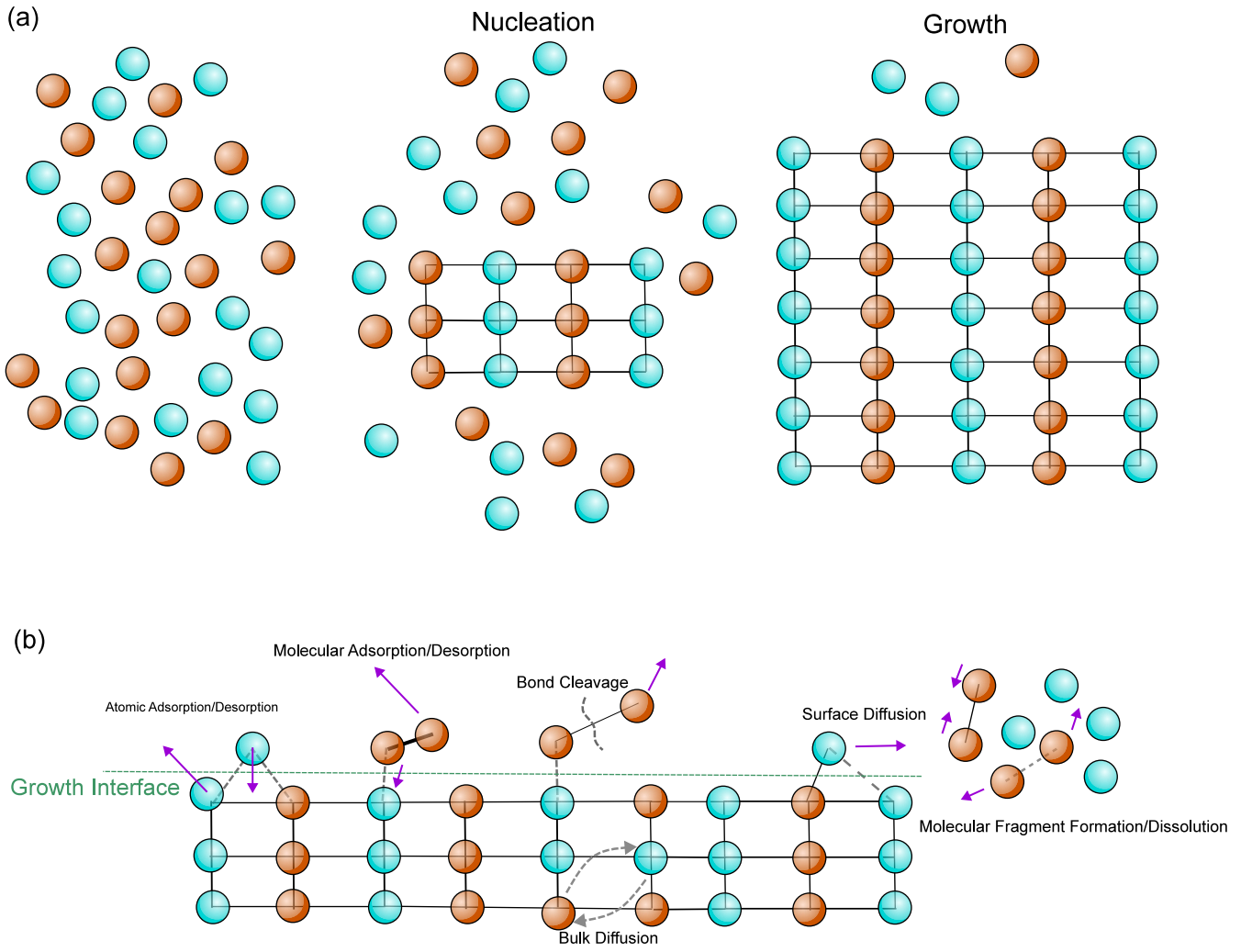

Figure 1. (a) Illustration of the two key steps of the crystal growth process. Initially, there is simply a collection of atoms with no defined order. Atomic rearrangement can happen here if needed, i.e., reaction between two or more reagents. The first step involves nucleation of a small crystal grain. The second step involves growth of the crystal grain into a larger bulk single crystal with defined order, removing free atoms from the system. (b) Key unsolved scientific challenges are related to how to control nucleation and growth and how to control the type, number, and distribution of defects in crystalline solids. These are in turn determined by the dynamical chemical reactions taking place at the interface between the solid and the fluid phase. There are many possible steps, including atomic and molecular adsorption/desorption, bond cleavage, and surface and bulk diffusion, further complicated by the formation of molecular fragments in the fluid phase. Together, these conspire to make it difficult to predict, in advance, the optimal crystal growth conditions for novel materials.

manufacture it on an industrial scale.[18,19] While the act of discovering these materials is itself a relatively difficult process, translating such discoveries from micron-scale to mm or larger scale is equally challenging and critical for practical exploitation. This is further complicated by the fact that it is defects, rather than the pristine material, which enable most functional behaviors, and defect type and concentration are frequently dependent on local growth conditions, including all of the kinetics factors mentioned above. Therefore, exploring avenues to control the type, number, and distribution of defects is important to make these defects work to our advantage.[20] Defect control can influence physical properties both by tuning desired properties and by introducing new physical properties.[21−25] Some of the many different types of defects relevant to a materials ultimate mechanical, optical, magnetic, and electronic behavior are shown in Figure 2.

As a result, single crystal growth is often considered "black magic", in which considerable time and resources are invested to optimize a material's growth and quality based on performance metrics, without a fundamental understanding of how the experimentally controllable parameters are changing the underlying thermodynamics and kinetics of the fluid−solid interface and driving the observed changes in defect types and distributions.

In this Review, we first describe a common set of single crystal growth methods often used within solid-state chemistry and materials physics, framed in the context of the control provided over known critical growth steps, while highlighting areas where crucial connections between control parameters and resultant material characteristics are not understood. These methods provide context for the types of control knobs available in practice, the types of materials that each technique excels at, and the types of defects one has more and less control over in each case. We then do a deep dive into the floating zone technique, pointing out innovations over the past decade that often take inspiration from these other methods and conclude with some remarks on future directions in crystal growth.

https://doi.org/10.1021/acs.chemmater.3c03077
Chem. Mater. 2024, 36, 4929−4944

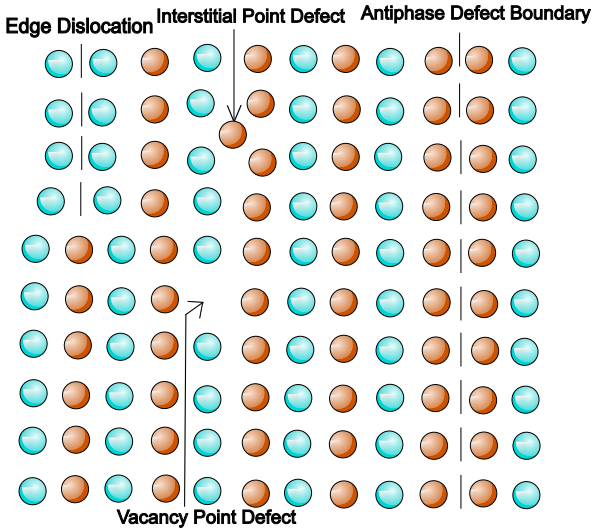

Figure 2. An ordered single crystal system, showcasing some of the many different types of defects that can occur in the structure and that impact the mechanical, electrical, optical, and magnetic properties of the material.

2. KEY CRYSTAL GROWTH TECHNIQUES

One of the more difficult choices to grasp for someone being introduced to the world of crystal growth is which technique to use for a particular reaction. Making a more optimal choice requires extensive knowledge and experience in understanding the starting reagents, the expected chemical behavior of the final product, and potential secondary reaction pathways. Furthermore, as there are many techniques and many ways a particular technique may fail to produce a good-quality crystal for the given application, it may not be immediately obvious to the novice that the choice of method is unsuitable for a specific material. Therefore, it is useful to understand some basic principles that form the foundation of crystal growth in order to avoid these situations.

Two universal experimental factors that determine the quality and feasibility of a crystal growth, aside from the particular behaviors of the starting and final materials, are the maximum temperature of the growth and the presence or absence of a solvent as part of the fluid phase.

Knowledge of the melting points of the starting reagents, or at least having a good estimate, is a crucial component of selecting an appropriate growth method, as different methods will comfortably accommodate different temperature ranges. For example, because vacuum arc melting uses an electric discharge to melt target materials, the temperatures involved can easily reach a few thousand degrees Celsius, and cooler temperatures below 1000 °C are difficult to produce in a controlled fashion. Relatedly, a basic but easily applicable method of crystal growth that can work well when the melting is congruent (i.e., the liquid has the same composition as the solid) is to melt a target material and, then cool it at a slow rate, forming crystals of the material as seeds randomly nucleate and grow during cooling. More involved methods attempt to control where nucleation occurs, where growth occurs, or both.

The choice of solvent is also important. It is first important note that there is no such thing as a solvent-free reaction: if no specific solvent is deliberately added, the material itself, in whatever fluid phase it exists, serves as its own solvent. The solvent has a significant impact not only on kinetics—by changing the molecular fragments that dynamically form and the mobility of the chemical species—but also on thermody-

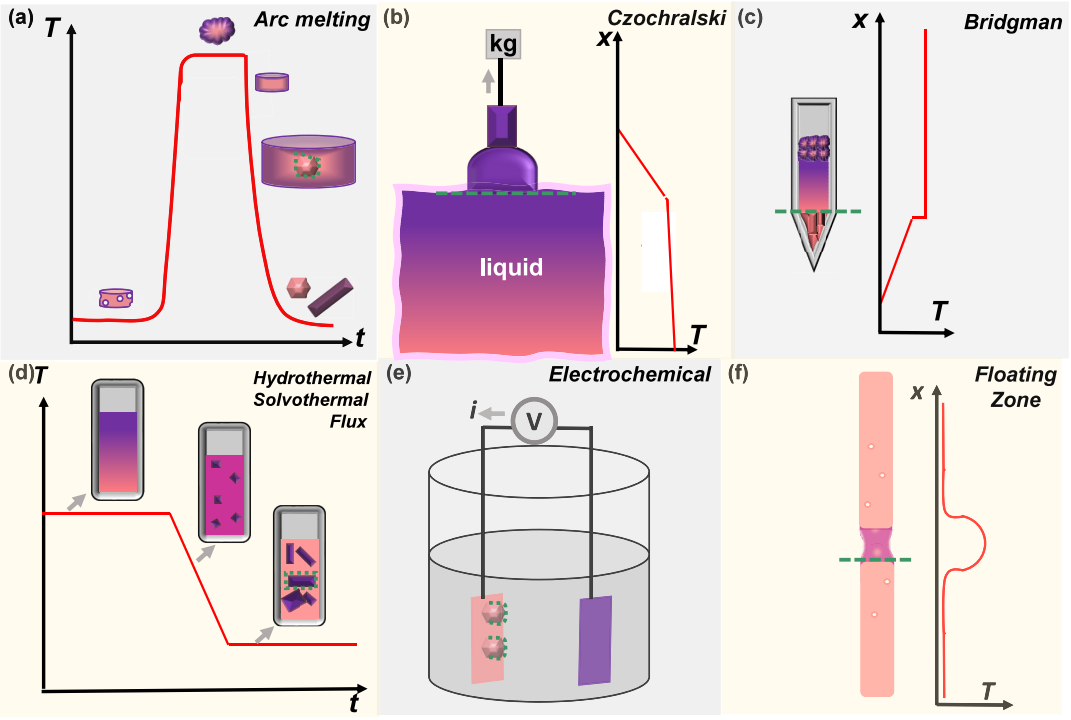

Figure 3. A number of synthesis techniques that are commonly utilized in solid-state chemistry, as well as where the growth interfaces are. More specifically (a) arc melting, (b) Czochralski method, (c) Bridgman method, (d) hydrothermal, solvothermal, and flux methods, (e) electrochemical crystal growth, and (f) floating zone growth. The green dashed lines indicate the solid−fluid interface at which growth is occurring in each case.

https://doi.org/10.1021/acs.chemmater.3c03077
Chem. Mater. 2024, 36, 4929−4944

Table 1. Summary of Common Crystal Growth Techniques in Materials Chemistry

	Flux Growth	Arc Melting	Hydrothermal	Bridgman Growth	Czochralski Growth	Electrochemical Solvothermal	Optical Floating Zone
Crystal Size	0.1 mm−5 cm	1 mm−10 cm	1 μm−1 mm	5 mm−20 cm	5 mm−20 cm	1 μm−1 mm	5 mm−10 cm
Material Compatibility	Determined by flux	Nonvolatile metals, oxides	Determined by water solubility	Most	Most	Soluble in chosen solvent	Absorbs directed light
Temperature	300−1250 °C	1500−3500 °C	100−800 °C	1000−2000 °C	300−3000 °C	100−500 °C	1000−2500 °C
Pressure	10^{-6}−100 bar	10^{-6}−3 bar	1−2500 bar	10^{-6}−100 bar	10^{-6}−100 bar	1−2500 bar	10^{-6}−8000 bar
Preparation Time	Minutes−Hours	Seconds−Minutes	Minutes−Hours	Minutes−Hours	Hours−Days	Minutes−Hours	Hours−Days
Growth Speed	Days−Months	Seconds−Minutes	Days−Months	Hours−Months	Hours−Months	Days−Months	Hours−Months
Sample Recovery	Centrifugation, Flux Dissolution	Direct	Filtration	Direct	Direct	Filtration	Direct
Likely Defects	Grain boundaries, Inclusions, Substitution	Vacancies, Internal strain	Vacancies, Solvent inclusion	Grain boundaries, vacancies	Grain boundaries, vacancies	Vacancies	Grain boundaries, vacancies
Chemical Control	Choice of flux	Limited by volatilization	Water solubility	Molten phase composition	Gas presence, Molten phase purity	Electrical conductivity, solubility	Gas flow, optical absorptivity

namics by, e.g., changing the rate at which volatilization or loss of chemical species occurs. A tried-and-true method using separately chosen solvents is the exploitation of a material's solubility to produce crystals by supersaturation, where the target material is dissolved in a chosen solvent to the point of supersaturation and then allowed to crystallize as the solution comes out of the supersaturated state. It is usually desirable for the solvent to be unreactive to the final product and to the formation of other phases, in order to prevent competing reaction pathways.

In addition to these two crucial experimental considerations, there are more method-specific considerations. The choice of heating method imposes constraints on which materials are possible to heat, as well as on the degree of control over the spatial and temporal variations in temperature (a critical thermodynamic variable). For example, induction heating cannot be used to directly heat insulating oxides since they do not meaningfully absorb in the radiofrequency regime. The use of electric discharges can provide massive temperatures but at the cost of fine control, especially at lower temperatures. The choice of container (crucible) to hold the reaction imposes similar constraints as it must be unreactive toward the material and solvent being used for growth.

These examples and principles, although by no means exhaustive, are intended to give the newcomer a glimpse of the relatively complex decision-making involved in selecting a crystal growth method. A great number of factors can influence the process and outcome of a crystal growth, some of which may not be easily controllable. However, it is possible to make a more optimal choice of method based on an educated deduction, taking into account the physical and chemical behavior of the material(s) in question, and improve the chances of success.

There are a wide variety of material classes and a similar range of available methods for high-quality crystal growth. Selected methods are summarized in Figure 3 and Table 1 and discussed here in turn. Additionally, a list of selected materials that can be crystallized by the methods discussed is presented in Table 2.

2.1. Arc Melting. Arc melting uses a high-voltage generator to generate an electric arc that is used as a direct heat source to melt materials such as refractory elements or compounds together to achieve reaction, as shown in Figure 3a.[26] Arc melting can usually directly melt target materials because it can reach extremely high temperatures ($T \sim 3500$ °C). Many materials targeted for synthesis via arc melting are intermetallic compounds, such as high-entropy[27,28] alloys, and even oxides and nitrides.[29,30] It is not normally considered a source of single crystals because it is "uncontrolled" cooling of a melt and does not exhibit specific control over either the nucleation or growth steps. However, this uncontrolled crystallization is still crystallization, and it is often possible to pull 10−100 μm scale single crystals from an arc melted boule. Further, it is the canonical method by which very large cubic zirconia single crystals used in, e.g., jewelry, are produced.[31] This works by melting a large volume of Y_2O_3-doped ZrO_2. When the arc is removed, the outside freezes rapidly forming a zirconia "shell" around a molten core. This shell has a low thermal conductivity and thus provides a protective shield that allows the majority of the material to exhibit convective flows, limiting the formation of nucleation sites and instead promoting the formation of large single crystals inside the shell.

Arc melting is one of the primary techniques used in the synthesis of medium- and high-entropy alloys, which are seeing significant interest for high temperature applications as well as corrosion resistance. One example of these materials synthesized by arc melting is NbMoTa.[32] An equiatomic mixture of elemental powders was pressed into a cylinder which was then arc-melted five times, inverting the ingot before each melt, in order to achieve homogeneity. This ingot was compared with an alloy of the same composition that was synthesized using the laser metal deposition method, in which homogenized metal powders were vaporized and deposited on a heated substrate, in order to determine how the different production methods influence the mechanical properties, microstructure, and phase composition. It was found that the arc-melted alloy has improved experimental yield and compressive strength at high temperature compared to the laser-deposited alloy, primarily due to defects arising from a steep temperature gradient inherent in the laser deposition process.

Excellent reviews going through the details of using arc melting for crystal growth are available.[33,34]

2.2. Czochralski. Czochralski growth is a method famously used for growing extremely large boules of single crystal semiconductor elements such as silicon.[9] For the typical growth, a large amount of the target material is completely melted in a crucible and is not spontaneously nucleating new

https://doi.org/10.1021/acs.chemmater.3c03077
Chem. Mater. 2024, 36, 4929−4944

Table 2. Selection of Different Materials That Can Be Crystallized by the Corresponding Growth Methods

	Oxides	Intermetallics	Nitrides	Sulfides	Halides
Floating Zone	Most metal oxides[100]	RuAl, TiAl, TiAlNb, Mn_3Si, TiNb[101]	Li_3N,[102] NbN-NbC binaries,[103] Cr_2N,[104] TiN, ZrN[105]	CdS[106]	NaCl, KCl, KBr, KI, LiF[107]
Flux Growth	Most metal oxides[1,108−111]	AV_3Sb_5,[67] $EuGa_2Sb_2$[68]	h-BN,[70] GaN,[112] Multicomponent nitrides[113]	ZnS,[114] $NaCrS_2$, $NaInS_2$, CdS[66]	Eu_4OCl_6, Eu_4OBr_6,[115] Tl_2MX_7 (M = La, Hf; X = Cl, Br; n = 5, 6)[116]
Arc Melting	$CeMO_3$ (M = Al, Ga),[117] $Zn_3Ta_2O_8$[29]	Rare earth and transition metal intermetallics,[118−121] Medium- and high-entropy alloys[27,32]	BN,[122] VN,[30] AlN[123]	$Zr_{3+x}S_4$,[124] Hf_2S[125]	
Bridgman	$Y_3Al_5O_{12}$,[44] β-Ga_2O_3,[126] ZnO[127]	CdTe, CdZnTe[128]		GaS,[47] $AgGaS_2$,[129] Bi_2S_3,[130] ZnS, CdS[131]	$KCaI_3$,[45] Alkaline earth mixed halides,[132] Ternary alkali lead halides[133]
Czochralski	$BaTiO_3$, TiO_2,[134] β-Ga_2O_3,[135,136] $Y_3Al_5O_{12}$,[135] $Gd_3Ga_5O_{12}$,[136] $LiAlO_2$,[137] $(La,Sr)(Al,Ta)O_3$[138]	GaSb,[139] Rare earth tetraborides[140]	Li_3N[141]	ZnS, CdS[131]	Rare earth halides,[142] KCl,[143] BaBrCl,[144] $BaMgF_4$[135]
Hydrothermal	ZnO,[11] WO_3,[145] Transition metal oxides[54,55,145−147]	$FeSn_2$,[148] IrRu,[149] Pd_3Pb,[150] SnSe[151]	VN,[152] BN,[153] GaN[53]	ZnS,[11] CdS,[154] Co_2RuS_4,[155] NiS, Co_9S_8[156]	$CsPb_2Cl_5$,[157] $CsPbBr_3$,[158] Rb_2SeOCl_4*H_2O,[159] $CsPb_2(Cl_{1-x}Br_x)_5$[157]
Solvothermal	Perovskite-structured oxides[160]	Binary Pt-based, Pd-based, and NiCo nanocrystals,[161] Pt_2In_3[60]	Ta_3N_5, TaN, MN (M = Zr, Hf, Nb),[162] Cu_3N[163]	CdS,[164] $CdIn_2S_4$[165]	$CsPbX_3$ (X = Cl, Br, I),[166] $CsSnX_3$ (X = Cl, Br, I)[167]
Electrochemical	Sc_2O_3,[168] Cu_2O[169]	Sm−Co magnets,[81] Bi_2Te_3,[170] Pd, HgPd, In_7Pd_3[171]	Zn_3N_2 thin film,[172] GaN,[173] SiCN[174]	Cu−Zn−S films,[175] FeS, $Fe_{1+x}S$ ($x \leq 0.11$)[176]	(BEDT-TTF)$Au(C_6Cl_5)_2$[82]

crystallites. A small single crystal seed is lowered into the melt to form a well-defined fluid−solid interface at the top of the melt and then pulled out at a very slow rate. The molten material crystallizes as it is removed from the heat, near the top of the liquid melt, ideally taking on the same crystallographic orientation as the seed that was used to begin the growth and forming a very large single crystalline domain, as shown in Figure 3b.[35] This technique has also been used in the growth of laser materials[36] and scintillators.[37] The growth of single crystal silicon via the Czochralski method is one of the most important accomplishments in crystal growth in the modern era and showcases the usefulness of crystal seeding and directional control of the solidification front in the growth process.[38] By dipping a small single crystal of silicon into a large pot of the molten material and then slowly pulling the seed out from the melt, a sharp temperature gradient is created which strongly encourages crystallization at the solid−liquid interface, and the pull gives a direction to the crystallization. Additionally, the small crystal serves as a nucleation point, which encourages formation of a single, larger crystal rather than multiple, smaller crystals. The slow pull maintains the connection between the growing crystal and the melt, while the newly formed single crystal takes on the orientation of the initial seed. This point is particularly useful if a specific crystal plane orientation is required. A significant limitation of this technique in a research context is the large molten volume required, which requires significant power input to create and maintain. Further, beyond the temperature gradient and degree of pot mixing, it is difficult to control parameters that affect the type and distribution of defects that form during the solidification process.

The gradual improvement of silicon crystal growth via the Czochralski method has been one of the most important for the development of modern technology and electronics, which are dependent on high-quality silicon in order to function effectively.[38] As such, a significant amount of research has gone into reviewing the development of and improvement of the methodology, as well as controlled introduction of defects into the single crystal. Typically, these take the form of dopants, creating substitution defects in the crystal, and are introduced by preparing an alloy of the desired dopant plus silicon with a uniform concentration of the former throughout. Alternatively, the dopant may be introduced directly to the melt. These dopants are typically used to influence the electrical properties of the silicon for different applications. For example, in a recent paper on doping Si electrodes for use in next-generation Li-ion batteries, doping Si with 2000 ppm of P enabled significantly increased electrical conductivity as well as improved reversible charge capacity. The phosphorus dopant was introduced by melting it simultaneously with the polycrystalline silicon reagent and then growing the crystal.[39]

Excellent reviews going through the details of using Czochralski for crystal growth are available.[40−42]

2.3. Bridgman-Stockbarger. Bridgman-Stockbarger, or colloquially just Bridgman, crystal growth moves the target material through a static hot zone, with crystallization occurring at a well-defined position where the temperature gradient is designed to be particularly sharp to traverse from a few degrees above to a few degrees below the melting point.[7,8] To help control initial nucleation, a pointed crucible is often used, ensuring that nucleation begins in a very small volume of the sample. The rate of movement is typically slow, in the order of millimeters per hour. A generic Bridgman crystal

https://doi.org/10.1021/acs.chemmater.3c03077
Chem. Mater. 2024, 36, 4929−4944

growth is shown in Figure 3c. There are multiple methods of generating the hot zone; one method is the induction method, which is useful when the target material is metallic or semiconducting. A large AC electric current is run through coils of conducting wire, which induces a current through the target material. The material then heats and melts via resistive heating. Bridgman growth can also take advantage of zone refinement purification, as impurities in the bulk material tend to stay in the liquid phase. Some of the first materials grown using this method include elemental crystals by Bridgman[7] and lithium fluoride by Stockbarger.[8] Recently, this technique has become primarily useful for slow, large crystal growth of both intermetallics[43] and oxides.[44] The single crystal growth of the $KCaI_3$:Eu scintillator by a self-seeding method[45] illustrates how nucleus selection can be used to enhance the crystal growth capabilities of a technique. In the traditional Bridgman technique, the whole material is melted and resolidified. This can produce large, high-quality single crystals due to the sharp temperature gradient involved and the large quantity of material, but typically, the initial nucleation step is uncontrolled; thus, the crystal domain is generally randomly selected for growth. If there are multiple crystal domains present in the solidifying material, more than one can be selected for growth, leading to a large crystal that is not perfectly a single domain throughout.[46] For scintillator materials, this is highly undesirable as the resulting crystal must be a single domain and generally of high optical quality in order to be useful. The self-seeding variation of the technique involves the addition of a capillary section to the sealed reaction vessel. The decreased volume that initial crystallization can take place in facilitates competing crystal growth processes, which ultimately leads to significantly reduced nucleation and therefore a much better chance of growing a truly single-domain crystal.

The Bridgman technique is similar to Czochralski crystal growth in that it utilizes a form of directed solidification to accomplish the crystallization of the target material. Additionally, like Czochralski growth, it uses a static hot zone to melt the material. However, some major differences are that typically a vessel containing the material for crystal growth is slowly moved through the static hot zone, instead of pulling out from a molten pot. Bridgman growth is also additionally able to work with materials that melt incongruently by using a different material as molten solvent, a variation known as the traveling solvent Bridgman growth. This is a technique that Czochralski growth has difficulty with, as there is greater risk of the solvent material being incorporated into the single crystal. The static molten pot of material means that, in order to safely extract the target material as a crystal, the solution would need to be supersaturated first.

A useful material that has been recently grown via the Bridgman method is GaS, which is interesting for its electronic/optoelectronic properties in two-dimensional form as well as potential for useful optical applications in the mid-infrared region. The method by Ohashi et al. uses polycrystalline material sealed in a carbon-coated quartz ampule, with a travel rate of 0.5 mm/h.[47] This relatively low temperature crystal growth is highly amenable to the use of sealed quartz ampules, in order to provide an accessible vacuum environment and an easily made container for starting material.

Excellent reviews going through the details of using Bridgman-Stockbarger for crystal growth are available.[42,48,49]

2.4. Hydrothermal and Solvothermal. The hydrothermal and solvothermal methods are notably different from the crystallization methods discussed thus far. The most important distinction is that hydrothermal and solvothermal techniques take place, as the name implies, in a solvent, whereas all of the prior methods do not necessarily require such a medium for crystallization to proceed. As a result, the mechanism of crystallization is somewhat different, being reliant on supersaturation of the solvent with the target material to achieve crystallization rather than relying on directional solidification to nucleate and grow the crystal. A generic illustration of this method can be seen in Figure 3d.

Hydrothermal synthesis uses an aqueous solution, typically pressurized to have a boiling point greater than 100 °C, as a solvent.[50] The selection of different temperature and pressure conditions can greatly impact the species formed in solution and thus can influence the reaction outcome. At a high enough temperature and pressure, the reaction can be brought to a supercritical state which changes the properties of the solvent,[51] allowing for reactions that might not otherwise occur. These conditions also allow to some degree the use of materials that may otherwise have low solubility in water to grow crystals. Hydrothermal synthesis has been used to synthesize a large variety of materials[52] such as ZnO and ZnS[11] and GaN,[53] as well as a number of different transition metal oxides.[54,55]

The crystal growth of GaN illustrates how different routes to the same single crystal exist and how the choice of certain reaction conditions may influence other decision points in the technique.[53] Two different mineralizers were studied, using ammonia as the liquid medium, which differed in being either acidic or basic in solution. The basic mineralizers reduce the solubility of GaN but are less corrosive to the reaction vessel and are therefore simpler to set up and run overall, while the acidic mineralizers do not reduce GaN solubility but are significantly more corrosive to the container and need specialized inner liners to prevent breakdown. A trade-off must therefore be balanced between ease of reaction preparation and repeatability and improved reactivity.

A more general form of hydrothermal synthesis is to replace water with nonaqueous solvents or solvothermal synthesis. The choice of solvent is extremely important and significantly affects the production of the target material. Often used now in the preparation of metal−organic framework single crystals,[56] the method has a long history[57] and has been used to carry out novel solid-state chemical transformations, such as in the preparation of formally Ni^{1+} phases (e.g., $La_4Ni_3O_8$[58,59]). Other techniques exist that function using mechanisms similar to that of hydrothermal and solvothermal synthesis, but instead of using a liquid medium to carry dissolved material, they use a gaseous medium. These techniques include physical vapor deposition, where target materials are vaporized and deposited as crystals or as a crystalline film on a cold surface from the gas phase, and chemical vapor transport, where a volatile transport agent is reacted with the target material to get it into the gas phase; then, the target material is deposited as crystals in a growth zone via temperature gradient while the transport agent is recovered and remains in the gas phase. The synthesis of the intermetallic Pt_2In_3 by Jana and Peter is a good example of reductive solvothermal synthesis.[60] K_2PtCl_4 and $InCl_3{\cdot}xH_2O$ were used as reagents and mixed together in a small amount of tetraethylene glycol and then heated in a sealed, Teflon-lined autoclave for 24 h. The material is synthesized as nanoparticles instead of single crystals; this is not uncommon in hydrothermal and solvothermal syntheses given the comparatively

https://doi.org/10.1021/acs.chemmater.3c03077
Chem. Mater. 2024, 36, 4929−4944

modest temperatures, though there are also plenty of exceptions.[61−63]

Excellent reviews going through the details of using hydrothermal and solvothermal methods for crystal growth are available.[64,65]

2.5. Flux. The flux growth method is like solution crystal growth in that materials are combined in a container and dissolved to facilitate the reaction.[13,15,16] The mechanism of crystal formation is shown in Figure 3d; it is similar in mechanism to the hydrothermal/solvothermal techniques. The flux, however, is typically some kind of solid that has a low melting point instead of a liquid solvent. The most important aspect of the chosen flux is that it should be able to dissolve all the reagents in order to facilitate the reaction between them, while also having large variations in solubility with temperature so that the condition of supersaturation can be produced. After the reaction is complete, the flux is typically slowly cooled to just above its melting point and then centrifuged in order to remove the excess flux. There are a wide variety of materials used as fluxes for this type of crystal growth, and many different materials have been crystallized using this technique[1,3,4] such as oxides,[1,14] sulfides,[66] and antimonides.[67,68] Important considerations include the choice of crucible material (it must be unreactive toward both the flux and dissolved species) and the binary/ternary/quaternary phase diagrams which dictate under what conditions the liquid is in equilibrium with the desired solid product. The growth of the kagomé crystal lattices KV_3Sb_5, RbV_3Sb_5, and CsV_3Sb_5 using the flux technique provides a convenient example of the entirety of the crystal growth process. The crystal is grown by combining the individual elements and using a melt eutectic of KSb_2 and either KSb or Sb as the flux medium.[67] The slow cooling process encourages a low level of nucleation and subsequently larger crystal growth. However, inclusions of the flux can occur in crystals formed using this technique. Furthermore, while flux adhering to the surface of a material may be easy to spot and, depending on the flux, easy to remove, inclusions in a crystal may not be as simple to spot as taking a look at the surface and often cannot be removed from the crystal. As such, it is important to screen crystals for inclusions. Recent developments in laboratory instrumentation and usage have led to more elegant ways to screen crystals. In particular, the emerging use of the X-ray microcomputed tomography technique has strong potential for *in situ* and postsynthesis screening and analysis, both for inclusions of extraneous material as mentioned previously as well as defect formation and crystal quality analyses.[69]

Hexagonal boron nitride, or h-BN, is a well-known and frequently studied two-dimensional material, particularly for use as substrates and protective layers over other two-dimensional materials and in a variety of next-generation devices. h-BN also possesses favorable and useful electric and chemical properties that further enhance its potential. As such, high-quality h-BN single crystals are in significant demand. Flux growth represents a relatively simple synthetic method by which these high-quality single crystals can be made, and a number of different one- and two-component fluxes have been successfully used to synthesize h-BN crystals. However, many of these fluxes have limitations, chiefly either the need for high pressure or the small size of the resulting crystals. In a recent paper by Edgar et al., these limitations are overcome by using a liquid iron flux with low carbon content. By dissolving boron powder and nitrogen gas into molten iron at 1550 °C and then slowly cooling to 1450 °C before quenching, large h-BN crystals with a maximum observed surface area of 4 cm^2 were precipitated on the surface of the iron flux.[70]

Excellent reviews going through the details of using flux methods for crystal growth are available.[71−75]

2.6. Electrochemical Synthesis. An electrochemical force can be used to drive formation of the desired phase,[76] as shown in Figure 3e. Long used for production of electroactive elements such as aluminum (the Hall-Héroult process[77,78]), it has also been used to great effect in the preparation of single crystals of novel molecular-based quantum phases.[79] A key strength of electrochemical methods is that they allow precise control over the thermodynamic driving force of formation and enable creation of oxidation states that are otherwise broadly inaccessible in single crystalline form. It further provides unique experimental handles through which to control nucleation and growth, since nucleation starts at a well-defined electrode, and growth can proceed by continued deposition on these seeds, where the relevant oxidation states of the atomic/molecular species is formed *in situ* near the growth interface. One relatively unique limitation is that it works best for materials that are electrically conductive and able to support appropriate transmission of the electrochemical potential to the growth interface. As a result, the method typically only works for materials that are electrically conductive, as the applied electric potential is maximized at the interface between the conductive electrode and the usually less-conductive solution.

Electrochemical methods have also been useful in the synthesis of magnetic materials. Generation of magnetism via electrochemical chemistry has occurred both via synthesis of a magnetic material and by electrochemically doping existing materials which induces magnetic order.[80,81] Notably, a number of organic magnetic materials, including one that displays ferroelectricity, have also been made using electrochemistry.[82,83]

Excellent reviews going through the details of using electrochemical methods for crystal growth are available.[64,84,85]

2.7. Floating Zone and Directional Solidification. So far, all of the techniques discussed require the use of a container/crucible. Due to simple entropic considerations, this inevitably leads to some inclusion[86] of crucible atoms in the grown material (however small). The floating zone method allows for material growth in which the material is only in contact with itself, and no separate crucible in required. The basic setup is shown in Figure 3f, in which a small molten zone of the target material is formed between two solid rods of the same material. This liquid region, held in place due to its own surface tension, "floats" in space, hence the name "floating zone". One rod functions as the "seed" rod, which serves as the platform on which the single crystal grows. The other rod functions as the "feed" rod, which feeds the target material into the molten floating zone, facilitating growth. As the liquid zone is moved in location relative to the rods (either by translating the rods or the heat source or both), material that was solid is turned into liquid, and material that was liquid turns into solid (i.e., directional solidification). This sets up a very well-defined solid−fluid interface at which crystallization occurs. In addition to enabling extreme purity due to the lack of a container, the floating zone approach also helps with practical considerations such as heat load and volatilization, since only a small portion of the material is in the fluid phase at a time.

https://doi.org/10.1021/acs.chemmater.3c03077
Chem. Mater. 2024, 36, 4929−4944

Similar to the Bridgman method, the floating zone functions using a static hot zone to melt materials and crystallizes the target using directional solidification. However, unlike the other directional solidification methods, the floating zone cannot control the crystalline nucleus selection as easily, as there is no simple capillary shape to use. One method sometimes used involves "necking" the molten zone by making it thinner, which accomplishes the same rapid selection of a single crystalline domain as the capillary point does for the Bridgman technique.

The heat source can be a variety of choices, including an electron-beam or induction melting, but one of the most popular, the optical floating zone (OFZ) technique, utilizes focused light. Lamps, usually Xenon or Halogen, emit light that is then reflected and focused by elliptical mirrors to form the heated area in which the floating zone forms. This growth technique is popular because it is broadly applicable to many different materials and the equipment is easily transitioned between different target materials. Additionally, the crystals produced by OFZ growth are of sizes (mm to cm) that are usable for many condensed matter characterization techniques. It also provides comparatively easy optical access for *in situ* monitoring and control.

The growth of single crystal $SrVO_3$ using the laser diode optical floating zone method highlights key considerations. Previous attempts to grow single crystals via the floating zone technique use $SrVO_3$ in addition to $SrCO_3$ and V_2O_5 as the component materials for the compacted rods. However, there are significant disadvantages to using these materials. $SrCO_3$ releases CO_2 when heated, which bubbles out from the rod and causes empty pockets to form. Additionally, $SrCO_3$ and V_2O_5 have noticeably different melting points, at 1494 and 681 °C, respectively. This means that, even if the rod is heated homogeneously, the rod does not melt in the same manner and this can increase the chance of inhomogeneous crystal growth. However, using $SrVO_3$ and $Sr_2V_2O_7$ as component materials for the crystal growth under a forming gas atmosphere prevents this from happening, as carbon is not present in this scheme, and allows for direct conversion of $Sr_2V_2O_7$ to $SrVO_3$.[11]

3. DEEP DIVE INTO OPTICAL FLOATING ZONE

3.1. Common Challenges and Limits. Initial nucleation during OFZ occurs even before the rods begin to move at the static solid−liquid interface. This does not become apparent, however, until the molten floating zone moves away from its initial location, and the material on the seed rod that moves out of the molten zone permanently resolidifies. It can be difficult to directly control the pace of crystallization or what grain is selected for larger growth, but there are a few factors that the user directly controls that can influence this. For the rate of resolidification, control of the temperature gradient between the solid−liquid interface helps control how quickly crystallization occurs. A delicate balance must be struck here; if the resolidification occurs too quickly, many crystal grains will form and the single crystal quality will be lost. However, if the resolidification occurs too slowly relative to the feed of new material, the molten zone can expand and may become physically unstable. Thus, floating zone growths are typically performed with a sharp temperature gradient at the solid−liquid interface. The sharp temperature gradient ensures that the formerly molten material resolidifies quickly if the floating zone is held only slightly above the material's melting point. The development of laser floating zone techniques increases the sharpness of the temperature gradient at the growth interface due to the reduced surface area that is heated by the lasers compared to reflected light from the lamps.

However, the actual parameter that can be directly controlled to influence the temperature is the light source power. This only indirectly sets the temperature, which also depends on the sources of heat flow away from the molten zone (see below). Similarly, many of the other parameters that we can directly control in the floating zone, such as but not limited to the rotation and translation rates, do not have a direct quantitative relation to some of the thermodynamic and kinetic parameters of the actual growth, as the amount of processing going on at once is voluminous, Figure 4.

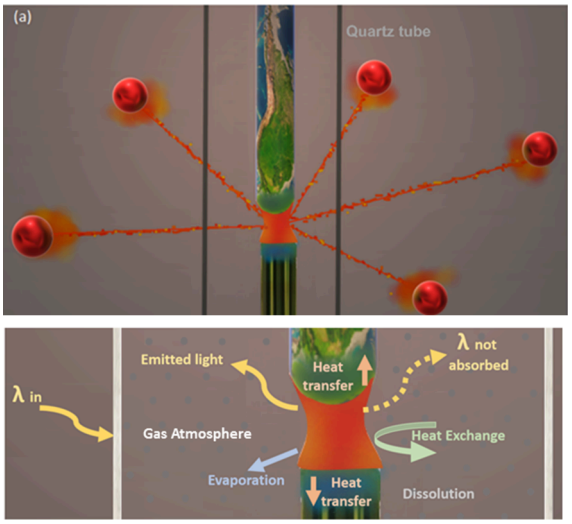

Figure 4. (a) Shows a traditional floating zone method that converts polycrystalline materials into phase pure single crystals. (b) This method can be thought of as the greenhouse effect that consists of the wavelength of light that enters to provide a heat source to create the molten zone and the avenues in which it undergoes heat sink and absorption. Illustrates some of the different interactions between the molten zone, the feed and seed rods, and the surrounding environment. During a floating zone crystal growth, the most readily controllable parameters are the power input, the environment (typically controlled by vacuum or gas flow), and translation/rotation of the two rods. However, there are other factors shown here influencing the crystal growth that are not directly controlled by these inputs. This shows how crystal growth is a complex affair and parameters within our control during the experiment do not necessarily influence some of the many different microscopic actions occurring at the same time.

One major example of a negative consequence of the indirect nature of control variables is the difficulty of precise temperature control of the molten zone. It is very difficult to measure the temperature of the molten zone because of the constraints of the experimental setup, precluding active feedback methods to enable a constant temperature in the face of varying zone volume or rod thermal properties. The most common optical method to measure temperature is to use a pyrometer to measure the blackbody radiation being emitted by the molten zone. However, there are two issues with this. First, pyrometers are not particularly accurate measurement tools, especially as they rely on emitted light and the lamps used for the optical floating zone, by nature, emit their own light which can interfere with the temperature measurement. Second, most useful synthetic databases do not

https://doi.org/10.1021/acs.chemmater.3c03077
Chem. Mater. 2024, 36, 4929−4944

usually contain information on a material's light absorptivity as a function of composition, which makes it nearly impossible to correctly set emissivity coefficients for more accurate measurement. Furthermore, the temperature of the molten zone is set by the power input, but this parameter does not have complete control over every factor in the floating zone setup that influences the final temperature of the molten zone, including not only radiative heat losses but also heat flow along the rods and losses with volatilizing species, combined with changes in surface area to volume ratio of the melt due to (small) variations in rod density or dimensions.

One potentially useful method for getting a better sense of the true temperature of the molten zone is to embed a thermocouple in one of the packed rods.[87] The thermocouple is thus placed much closer to the actual molten zone, in theory getting a better sense of the true temperature by proximity. However, there are still issues with this. First, engineering the packed powder rod itself and embedding a thermocouple in it is challenging. Second, because the thermocouple is simply placed near the molten zone, it can be influenced by the thermal conductivity of the material. Finally, any sections of the rod with the thermocouple embedded inside cannot be used for actual crystal growth, limiting the potential for large-scale single crystal growth with precisely controlled temperature.

A second challenge specific to OFZ is that the material to be grown must absorb the energy from the light providing the heating. In the case of broadband light sources, such has halogen or xenon bulbs, this is typically not an issue as most materials absorb some fraction of the spectrum. However, with the advent of laser techniques, this becomes a more crucial consideration. One solution is to add a small amount of a color center dopant to transparent materials to act effectively as an absorber. If the color center (due to entropic considerations) preferentially stays in the melt, not in the growing crystal, then it is possible to grow materials that do not absorb the wavelength of laser light used. This can also happen "natively"; e.g., in $Ba_2CaWO_{6-\delta}$, the single crystal growth is done utilizing 7 bar pressure of Ar for stabilizing the growth. Under these conditions, oxygen vacancies form that change the color from white to dark blue, enabling absorption of near-IR laser light.[22] To correct the oxygen vacancies in the grown crystal, the single crystal is then annealed under oxygen for a long duration of time to regain its white color. Another method to promote absorption is shading the outer region of otherwise non-absorbing crucibles (e.g., BN) with graphite to allow for light absorption and therefore successful heating, with the level of light absorption dependent on the amount of shading (darker shades will be better in light absorption—with the upper limit being the scenario of placing a BN crucible inside a C crucible).

3.2. Laser Pedestal (LPFZ). The laser pedestal technique was developed to enable growth of oxides with very high melting points by requiring melting of only a small portion of the total material.[88] This variant method functions by pulling out a single crystal from the melt on top of the "pedestal" and can also be performed in an OFZ furnace, Figure 5. Instead of generating a full molten zone connecting two solid rods, only the tip of a single rod is heated to create a molten pool on the top of the rod. A small piece of wire, or a seed crystal, is then inserted into the melt and slowly drawn out. Like in the Czochralski method, the material crystallizes at the top of the liquid as the molten material leaves the hot zone. Compared to

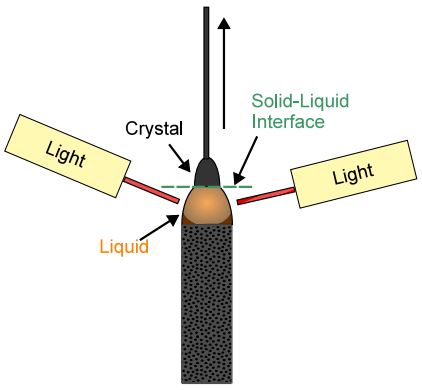

Figure 5. In the laser pedestal variant of the floating zone technique, a bottom polycrystalline seed rod is prepared and a melt formed on top as usual. Then, a thin wire or seed crystal is dipped into the melt from the top to form a solid−liquid interface at which controlled crystallization occurs as the wire is pulled up. At the same time, the bottom rod is slowly translated upward to keep a uniform molten zone volume. The result is crystallization is controlled as in the Czochralski method but in a more energy efficient way due to the small liquid volume that also avoids the challenges of crucible selection.

Czochralski, LPFZ reduces the energy requirements by reducing the total volume of material melted at one time. The melt is rotated at a constant speed counter to the rotation direction of the wire to stir the melt and produce a more homogeneous crystal. The slow draw speed out of the melt is facilitated by moving the wire and the rod in the same direction with the wire moving proportionally faster to ensure constant molten material volume. This variant technique is effective for materials that can be melted but has undesirable properties such as a low surface tension, incongruent melting behavior, or very high melting temperature. The pulling wire material must be carefully selected such that it will not dissolve in the melt. Here, the ability to tilt/angle the incident lasers becomes essential, because it permits use of a larger diameter "bottom" rod in which a pool of molten material can be produced with the material as its own crucible. This makes it a substantially easier to use version of a typical cold-crucible CZ/skull-melting process but with a similar ability to produce high purity and uniform materials, while being more energy efficient (since only a small portion of the material is melted at once).

An example of a material made via the laser pedestal variant technique is $YbIr_3Si_7$, synthesized by Stavinoha et al.[89] This material is interesting because of the simultaneous antiferromagnetic ordering and bulk insulating behavior, the former occurring at 4.1 K and the latter at >50 K. Furthermore, $YbIr_3Si_7$ possesses conducting surface states, in contrast to the bulk insulating behavior. The starting material for crystal growth was first prepared by arc melting stoichiometric amounts of the elements into a polycrystalline rod. The tip of the rod was melted using the laser heat sources, and a nickel−chromium wire was dipped into the melt to generate a seed crystal. The newly crystallized seed was pulled out of the melt at a slightly faster rate than the rod was fed into the melt, in order to facilitate the growth of the large bulk single crystal.

3.3. Flux-like Traveling Solvent Technique (TSFZ). The traveling solvent (TSFZ) technique uses principles from the flux crystal growth technique,[90] in the sense that the desired phase is dissolved in a solvent and then precipitated to

https://doi.org/10.1021/acs.chemmater.3c03077
Chem. Mater. 2024, 36, 4929−4944

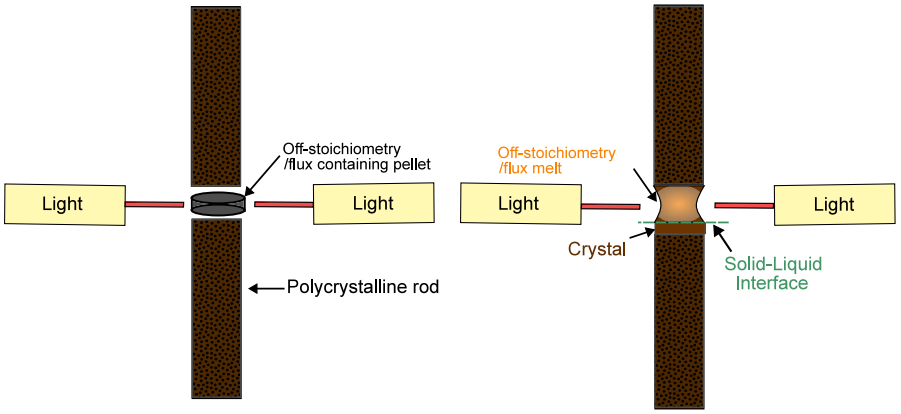

Figure 6. The traveling solvent floating zone (TSFZ) method utilizes a molten zone of a different stoichiometry than the target material to assist in floating zone growth. Usually, on-stoichiometry rods are used combined with a small pellet containing the flux/off-stoichiometry necessary to setup stable growth of the target material. A molten zone is then formed and translated as in the usual FZ method, but since the solid stable to precipitate at the solid liquid interface is the desired phase and since the composition of the melt is not changing in net due to feeding of new material from the top, the result is a stable precipitation from a solvent/off-stoichiometry melt.

grow large, pure single crystals of the target phase. In the TSFZ method, the solvent is usually packed as a pellet or sintered at the end of the seed rod. The molten zone that is formed then has a different composition from that of the seed or feed rods. If, at the temperature of the solid liquid interface, the stable solid to precipitate is the desired phase, then the target material crystallizes as in a standard floating zone crystal growth, Figure 6. This versatile technique has been used to tune the stoichiometry of quantum materials such as the pyrochlore oxides, e.g., $Yb_2Ti_2O_7$.[23] Another example is the growth of YbB_{12}, which requires use of a boron-rich flux and precise temperature control to maintain growth stability.[91,92]

3.4. Bridgman in Floating Zone. The Bridgman technique[93] is also possible in the floating zone environment due to the ability to form a static heating zone. Instead of moving the seed and feed rods at different speeds, simply moving both rods at the same speed and in the same direction through the static heating area allows for Bridgman-type crystal growth and zone refinement, Figure 7. This variant technique is more effective when using a laser OFZ furnace because of the greater precision of laser heating, since lasers can be focused on a smaller surface area compared to light from a bulb source. Furthermore, this method can be used where a traditional Bridgman crystal growth might not be possible, perhaps due to sensitivity of the material to oxygen or moisture, or it might be too volatile (as in $MgCo_6Ge_6$[94]), or the material may be insufficiently conducting but does absorb light well, rendering induction heating unsuitable.

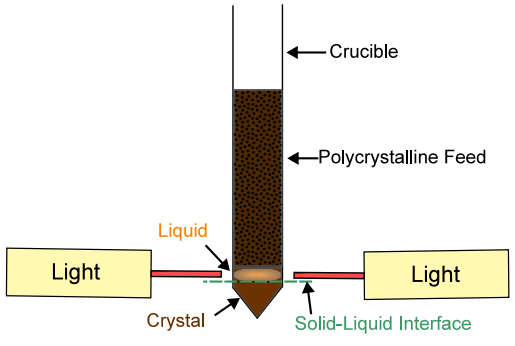

Figure 7. Setup for use of the Bridgman method in the floating zone. The FZ heating produces a narrow zone of molten material in between polycrystalline feed and single crystal seed regions. Growth occurs at the solid liquid interface as the crucible is translated down relative to the light sources. Either the crucible is transparent to the applied light and the sample absorbing, or vice versa. Because of the more limited volume of liquid present, this technique can succeed even when traditional Bridgman fails by allowing for higher temperatures, reduced vaporization, or both.

4. COMMON CONSIDERATIONS

4.1. Choice of Crucible. With the exception of the floating zone method, all the techniques described here involve reactions where the target phases are in direct contact with a container or crucible.

An ideal crucible is one that is inert toward the material being prepared; i.e., they are completely unreactive with each other and with the surrounding/contained fluid environment. This can, to a first approximation, be selected by consideration of the relevant binary phase diagrams and making sure there are no intermediate phases or that the temperatures required to start forming those phases (due to kinetics) is higher than the synthesis temperature.

Many different types of crucibles are often utilized in conventional solid-state chemistry synthesis. The most frequently used crucibles include alumina, graphite, boron nitride, fused silica, and metallic crucibles: W/Pt/Mo/Au/Ta/Nb. These crucibles provide secondary containment for reactants not to have parasitic oxides or unfavorable stable phases. A variation to these frequently used crucibles is alumina or fused silica with graphite lining or pencil shading to provide a protective inner layer. Sometimes using metallic foil packets instead of crucibles enables better coverage of the sample with less vaporization.

When some amount of reactivity is unavoidable, layered containers can be used. For example, fused silica recrystallizes in the presence of atmospheric moisture above ∼1050 °C, greatly diminishing structural integrity. Thus, using a secondary, sacrificial, outer fused silica ampule can allow for successful protection and use of the inner fused silica container up to ∼1300 °C. Another example is reusing prereacted crucibles to allow for formation of a self-determined passivating layer “empirically”.

https://doi.org/10.1021/acs.chemmater.3c03077
Chem. Mater. 2024, 36, 4929−4944

4.2. Repeated Seeding. Seeded growths involve the introduction of small crystal seeds into a reaction medium to encourage growth on that particular grain, similar to how Czochralski and Bridgman crystal growths use a seed crystal to encourage large crystal growth and the formation of a seed in a narrow space which encourages growth from the single crystal grain that outcompetes all others, respectively. Here, taking a small crystallite from initial growth attempts and reusing it with similar synthesis conditions can mimic this process, encouraging single crystal growth around the seed crystallite, reducing or eliminating the formation of additional nucleation sites. This technique, while reducing additional nucleation and encouraging grain growth on the single grain similar to the Czochralski technique, can lead to the formation of striations in the crystals from the repeated seedings.

4.3. Compositional Limitations. It is often stated that single crystals enable greater crystallographic perfection than polycrystalline methods, but this is often not the case. The reason is subtle but important: because single crystal growths occur at the interface between a fluid (liquid or gas) and a solid, i.e., in a two phase region of a phase diagram, it is not possible to freely control the stoichiometry of the growing crystal. Instead, the crystal is "pinned" to the composition that is in equilibrium with the fluid phase under the conditions of growth. This is illustrated for a hypothetical binary compound AB in Figure 8, where the stoichiometries accessible from a flux-based approach are highlighted in green and purple. More B-rich compositions, including the perfect 1:1 stoichiometry, are not in equilibrium with the liquid (highlighted in red) and therefore not directly accessible with single crystal growth.

There are no such restrictions when doing pure solid reactions, as in polycrystalline powders, where one can directly target any temperature and composition point in the phase diagram. As such, polycrystalline specimens can be, and in many cases are, more stoichiometrically perfect than their single crystal counterparts.

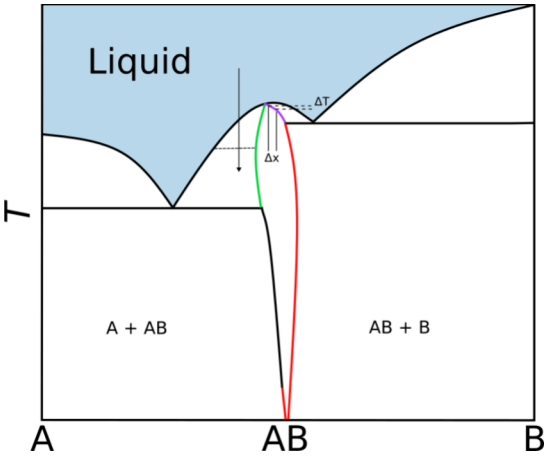

Figure 8. A hypothetical binary phase diagram illustrating the challenges of compositional control during single crystal growth. Direct melting can produce only a single composition—that of the point where the AB single phase region touches the liquid phase (the intersection of green, purple, and black lines). Changing to an A-rich melt enables one to access the compositions along the boundary of the liquid-AB region, highlighted in green. Using a more B-rich melt than the apex can form those compositions highlighted in purple. It is not possible, however, to access those compositions highlighted in red through a fluid−solid crystallization process because there is no two phase region including a fluid as the second phase. Even those compositions in purple are difficult to access in practice because a very small change in temperature (e.g., natural fluctuations) results in a large change in the composition of the solid precipitated.

In such cases, additional complexity must be added to the crystal growth method in order to access the exact desired stoichiometry. In the case of this flux example, this requires changing another thermodynamic variable (e.g., pressure) or adding another component in order to expose a region where the desired stoichiometry is in equilibrium with a fluid phase.

Even if the desired composition is found in equilibrium with a fluid, it may be extremely difficult to in fact produce a homogeneous stoichiometry because small variations can cause large changes in the equilibrium composition. This is shown for the compositions highlighted in purple, where a very small ΔT induces a large compositional change Δx. This adds a further constraint on the method used for growth.

5. AN OPEN FRONTIER: USING GRADIENTS IN CRYSTAL GROWTH

The use of temperature gradients in crystal growth is well-known, e.g., while executing the Bridgman and Czochralski techniques. However, gradients of pressure, concentration, and magnetic and electric fields, all of which have been utilized in the preparation of "semiconductor" grade single crystals,[20,95] can also be used. For example, concentration gradients can be seen in traditional dual solvent recrystallization techniques. The target material is dissolved in a solvent to the point of saturation; then, a second solvent, in which the target material is both not present and insoluble, is carefully layered on top of the saturated solution. Over time, the two solvents mix, and the target material crystallizes out of solution. Concentration gradients are also used in flux crystal growths similarly to traditional solvent recrystallization, with the target material growing in areas of supersaturation within the flux.[95]

Nonstandard gradients can be used to improve crystal growth by drawing impurities within the target material toward one end of the gradient, resulting in a more pure single crystal that may potentially have fewer defects by removing inclusions and other disruptions to the regular structure. This is most viable when there are significant differences in the physical properties of the target material and the known or suspected impurities, such as if the impurities are magnetic or electrically conductive and the target material is nonmagnetic or electrically insulating. For example, during an induction Bridgman growth, an electric current is induced in the target material which heats and eventually melts it. If there is an impurity phase which couples better than the target material with the applied current, it will remain in the melt while the rest crystallizes. Alternatively, it is possible to draw impurities to different areas of a solution using electric or magnetic fields, given that the impurity phase(s) and the target material respond differently, for example, if the target material is nonmagnetic while the impurity phase is attracted to the field. These effects occur even when the energy content of the applied field (e.g., 1 T magnetic field ∼1 K of energy) is much less than the growth temperature.

External applied pressure has been used in a number of different applications for material synthesis. Pressure gradients can have varying effects. For example, AgI is shown to eventually dissociate under applied pressure.[96] In terms of crystal growth, pressure gradients can be created as a result of the primary applied temperature gradient which then

https://doi.org/10.1021/acs.chemmater.3c03077
Chem. Mater. 2024, 36, 4929−4944

encourages crystal formation. For example, in physical vapor deposition and chemical vapor transport methods, a partial gas pressure composed of the gaseous target material or gaseous intermediate is generated at one end of the reaction chamber. This gas is immediately part of a pressure gradient across both ends of the chamber, following the applied temperature gradient. As the gas travels down the length of the chamber, the applied temperature gradient reduces the maximum vapor pressure of the gaseous material to the point where the maximum falls below the present vapor pressure at the cool end of the chamber, which causes crystal growth.

6. SUMMARY

Several techniques for the synthesis of new materials, both common and uncommon, have been presented with a special focus on how each technique tackles the single crystal growth process differently and how variations on the established methods alter the standard process to enable and/or improve specific parts of the growth process. Additional synthetic techniques in the scientist's toolkit provide improved flexibility[97−99] in the number of routes to approach the crystal growth of any one material, which can help synthesize single crystals of materials that might otherwise be unsuitable for certain techniques, and therefore improves the ability to target many more classes of materials for research. With greater visibility, it is hoped that greater usage and throughput for new and interesting materials in order to push forward on the many challenges facing society today will come.

■ ASSOCIATED CONTENT

Data Availability Statement

Additional data associated with this account is available at 10.34863/w4qs-f408.

■ AUTHOR INFORMATION

Corresponding Authors

Tanya Berry − *Department of Chemistry, Princeton University, Princeton, New Jersey 08544, United States;* orcid.org/0000-0002-1583-2120; Email: tberry@princeton.edu

Nicholas Ng − *Department of Chemistry, The Johns Hopkins University, Baltimore, Maryland 21218, United States; Institute for Quantum Matter, William H. Miller III Department of Physics and Astronomy, The Johns Hopkins University, Baltimore, Maryland 21218, United States;* orcid.org/0000-0002-3635-8309; Email: nng3@jhu.edu

Tyrel M. McQueen − *Department of Chemistry, The Johns Hopkins University, Baltimore, Maryland 21218, United States; Institute for Quantum Matter, William H. Miller III Department of Physics and Astronomy and Department of Materials Science and Engineering, The Johns Hopkins University, Baltimore, Maryland 21218, United States;* orcid.org/0000-0002-8493-4630; Email: mcqueen@jhu.edu

Complete contact information is available at: https://pubs.acs.org/10.1021/acs.chemmater.3c03077

Notes

The authors declare no competing financial interest.

■ ACKNOWLEDGMENTS

T.B. acknowledges support from NSF-MRSEC through the Princeton Center for Complex Materials NSF-DMR-2011750. T.M.M. and N.N. acknowledge support by the National Science Foundation (Platform for the Accelerated Realization, Analysis, and Discovery of Interface Materials (PARADIM)) under Cooperative Agreement No. DMR-2039380.

■ REFERENCES

(1) Bugaris, D. E.; zur Loye, H.-C. Materials Discovery by Flux Crystal Growth: Quarternary and Higher Order Oxides. *Angew. Chem., Int. Ed.* **2012**, *51* (16), 3780−3811.

(2) Schütz, M. B.; Xiao, L.; Lehnen, T.; Fischer, T.; Mathur, S. Microwave-assisted synthesis of nanocrystalline binary and ternary metal oxides. *Int. Mater. Rev.* **2018**, *63* (6), 341−374.

(3) Canfield, P. C.; Fisk, Z. Growth of single crystals from metallic fluxes. *Philos. Mag. B* **1992**, *65* (6), 1117−1123.

(4) Slade, T. J.; Canfield, P. C. Use of Refractory-Volatile Element Deep Eutectic Regions to Grow Single Crystalline Intermetallic Compounds. *Z. Anorg. Allg. Chem.* **2022**, *648*, No. e202200145.

(5) Schmidt, P.; Binnewies, M.; Glaum, R.; Schmidt, M. Chemical Vapor Transport Reactions-Methods, Materials, Modeling. *Advanced Topics on Crystal Growth.*; InTech, 2013.

(6) Binnewies, M.; Schmidt, M.; Schmidt, P. Chemical Vapor Transport Reactions-Arguments for Choosing a Suitable Transport Agent. *Z. Anorg. Allg. Chem.* **2017**, *643*, 1295−1311.

(7) Bridgman, P. W. Certain Physical Properties of Single Crystals of Tungsten, Antimony, Bismuth, Tellurium, Cadmium, Zinc, and Tin. *Proc. Am. Acad. Arts Sci.* **1925**, *60* (6), 305−383.

(8) Stockbarger, D. C. The Production of Large Single Crystals of Lithium Fluoride. *Rev. Sci. Instrum.* **1936**, *7*, 133−136.

(9) Zulehner, W. Czochralski Growth of Silicon. *J. Cryst. Growth* **1983**, *65*, 189−213.

(10) Tokita, M. Progress of Spark Plasma Sintering (SPS) Method, Systems, Ceramics Applications and Industrialization. *Ceramics* **2021**, *4* (2), 160−198.

(11) Laudise, R. A.; Ballman, A. A. Hydrothermal Synthesis of Zinc Oxide and Zinc Sulfide. *J. Phys. Chem.* **1960**, *64* (5), 688−691.

(12) Pistawala, N.; Rout, D.; Saurabh, K.; Bag, R.; Karmakar, K.; Harnagea, L.; Singh, S. Crystal growth of quantum materials: a review of selective materials and techniques. *Bull. Mater. Sci.* **2022**, *45*, 10.

(13) Schmehr, J. L.; Wilson, S. D. Active Crystal Growth Techniques for Quantum Materials. *Annu. Rev. Mater. Res.* **2017**, *47*, 153−174.

(14) Milisavljevic, I.; Wu, Y. Current status of solid-state single crystal growth. *BMC Mater.* **2020**, *2*, 2.

(15) Sales, B. Introduction to the Synthesis of Quantum Materials: Some General Guidelines and A Few Tricks. *Fundamentals of Quantum Materials* **2021**, 1−17.

(16) Kimura, S.; Kitamura, K. Floating Zone Crystal Growth and Phase Equilibria: A Review. *J. Am. Ceram. Soc.* **1992**, *75* (6), 1440−1446.

(17) Kim, J.; Kimura, Y.; Puchala, B.; Yamazaki, T.; Becker, U.; Sun, W. Dissolution enables dolomite crystal growth near ambient conditions. *Science* **2023**, *382* (6673), 915−920.

(18) Eagar, T. W. Bringing new materials to market. *Technology Review* **1995**, *98* (2), 42−49.

(19) Recatala-Gomez, J.; Suwardi, A.; Nandhakumar, I.; Abutaha, A.; Hippalgaonkar, K. Toward Accelerated Thermoelectric Materials and Process Discovery. *ACS Appl. Energy Mater.* **2020**, *3* (3), 2240−2257.

(20) Lin, W.; Benson, K. E. The Science and Engineering of Large-Diameter Czochralski Silicon Crystal Growth. *Annu. Rev. Mater. Sci.* **1987**, *17*, 273−298.

(21) Eo, Y. S.; Rakoski, A.; Lucien, J.; Mihaliov, D.; Kurdak, Ç.; Rosa, P. F. S.; Fisk, Z. Transport gap in SmB_6 protected against disorder. *Proceedings of the National Academy of Sciences USA* **2019**, *116*, 12638−12641.

(22) Sinha, M.; Pearson, T. J.; Reeder, T. R.; Vivanco, H. K.; Freedman, D. E.; Phelan, W. A.; McQueen, T. M. Introduction of spin centers in single crystals of $Ba_2CaWO_{6-\delta}$. *Phys. Rev. Mater.* **2019**, *3*, No. 125002.

(23) Arpino, K. E.; Trump, B. A.; Scheie, A. O.; McQueen, T. M.; Koohpayeh, S. M. Impact of stoichiometry of $Yb_2Ti_2O_7$ on its physical properties. *Phys. Rev. B* **2017**, *95*, 94407.
(24) Berry, T.; Bernier, S.; Auffermann, G.; McQueen, T. M.; Phelan, W. A. Laser floating zone growth of $SrVO_3$ single crystals. *J. Cryst. Growth* **2022**, *583*, No. 126518.
(25) Pressley, L. A.; Torrejon, A.; Phelan, W. A.; McQueen, T. M. Discovery and Single Crystal Growth of High Entropy Pyrochlores. *Inorg. Chem.* **2020**, *59* (23), 17251.
(26) Bradshaw, A. R.; Fort, D. A laboratory-scale arc furnace for melting volatile metals under elevated inert gas pressures. *Rev. Sci. Instrum.* **1992**, *63*, 5459.
(27) Joseph, J.; Jarvis, T.; Wu, X.; Stanford, N.; Hodgson, P.; Fabijanic, D. M. Comparative study of the microstructures and mechanical properties of direct laser fabricated and arc-melted $Al_xCoCrFeNi$ high entropy alloys. *Mater. Sci. Eng., A* **2015**, *633*, 184−193.
(28) Sharma, A.; Oh, M. C.; Ahn, B. Microstructural evolution and mechanical properties of non-Cantor AlCuSiZnFe lightweight high entropy alloy processed by advanced powder metallurgy. *Mater. Sci. Eng., A* **2020**, *797*, No. 140066.
(29) Yajima, R.; Kamada, K.; Takizawa, Y.; Yoshino, M.; Murakami, R.; Kim, K. J.; Horiai, T.; Yamaji, A.; Kurosawa, S.; Yokota, Y.; Sato, H.; Toyoda, S.; Ohashi, Y.; Hanada, T.; Yoshikawa, A. Growth of $Zn_3Ta_2O_8$ crystal scintillator by a novel melt growth technique named shielded arc melting method. *Opt. Mater.: X* **2022**, *14*, No. 100149.
(30) Tripathy, P. K.; Arya, A.; Bose, D. K. Preparation of vanadium nitride and its subsequent metallization by thermal decomposition. *J. Alloys Comp.* **1994**, *209*, 175−180.
(31) Fisher, G.; Seacrist, M. R.; Standley, R. W. Silicon Crystal Growth and Wafer Technologies. *in Proceedings of the IEEE* **2012**, *100*, 1454−1474.
(32) Li, Q.; Zhang, H.; Li, D.; Chen, Z.; Wang, F.; Wu, M. Comparative study of the microstructures and mechanical properties of laser metal deposited and vacuum arc melted refractory NbMoTa medium-entropy alloy. *Int. J. Ref. Met. Hard. Mater.* **2020**, *88*, No. 105195.
(33) Boxman, R. L.; Goldsmith, S.; Greenwood, A. Twenty-five years of progress in vacuum arc research and utilization. *IEEE Trans. Plasma Sci.* **1997**, *25* (6), 1174−1186.
(34) Jones, D. W. Refractory Metal Crystal Growth Techniques. In *Crystal Growth Theory and Techniques*; Springer, 1974; Vol. 1.
(35) Czochralski, J. Ein neues Verfahren zur Messung der Kristallisationsgeschwindigkeit der Metalle. *Z. Phys. Chem.* **1918**, *92U* (1), 219−221.
(36) Asadian, M.; Hajiesmaeilbaigi, F.; Mirzaei, N.; Saeedi, H.; Khodaei, Y.; Enayati, S. Composition and dissociation processes analysis in crystal growth of Nd: GGG by the Czochralski method. *J. Cryst. Growth* **2010**, *312*, 1645−1650.
(37) Nikl, M.; Yoshikawa, A. Recent R&D Trends in Inorganic Single-Crystal Scintillator Materials for Radiation Detection. *Adv. Opt. Mater.* **2015**, *3* (4), 463−481.
(38) Lomonova, E. E.; Osiko, V. V. Growth of Zirconia Crystals by Skull-Melting Technique. In *Crystal Growth Technology*; Scheel, H. J.; Fukuda, T.Eds.; John Wiley & Sons Ltd, 2003; ISBN: 0-471-49059-8.
(39) Shimizu, M.; Kimoto, K.; Kawai, T.; Taishi, T.; Arai, S. Dopant Effect on Lithiation/Delithiation of Highly Crystalline Silicon Synthesized Using the Czochralski Process. *ACS Appl. Energy Mater.* **2021**, *4* (8), 7922−7929.
(40) Baumbach, R. E. Induction Furnace Heating for Growth of Intermetallic Quantum Materials. In *Fundamentals of Quantum Materials: A Practical Guide to Synthesis and Exploration*; World Scientific Publishing, 2021.
(41) Yoshikawa, A.; Chani, V.; Nikl, M. Czochralski Growth and Properties of Scintillating Crystals. *Acta Phys. Polo. A* **2013**, *124* (2), 250−264.
(42) Pistawala, N.; Rout, D.; Saurabh, K.; Bag, R.; Karmakar, K.; Harnagea, L.; Singh, S. Crystal growth of quantum materials: a review of selective materials and techniques. *Bull. Mater. Sci.* **2022**, *45*, 10.
(43) Cheuvart, P.; El-Hanani, U.; Schneider, D.; Triboulet, R. CdTe and CdZnTe Crystal Growth by Horizontal Bridgman Technique. *J. Cryst. Growth* **1990**, *101*, 270−274.
(44) Petrosyan, A. G. Crystal growth of laser oxides in the vertical Bridgman configuration. *J. Cryst. Growth* **1994**, *139*, 372−392.
(45) Lindsey, A. C.; Wu, Y.; Zhuravleva, M.; Loyd, M.; Koschan, M.; Melcher, C. L. Multi-ampoule Bridgman growth of halide scintillator crystals using the self-seeding method. *J. Cryst. Growth* **2017**, *470*, 20−26.
(46) Triboulet, R. CdTe and CdZnTe Growth. In *Crystal Growth Technology*; Scheel, H. J.; Fukuda, T., Eds.; John Wiley & Sons Ltd. 2003; ISBN: 0-471-49059-8.
(47) Nakamura, M.; Nakamura, H.; Shimamura, K.; Ohashi, N. Growth and characterization of a gallium monosulfide (GaS) single crystal using the Bridgman method. *J. Cryst. Growth* **2021**, *573*, No. 126303.
(48) Capper, P. Bulk Crystal Growth: Methods and Materials. In *Springer Handbook of Electronic and Photonic Materials*; Springer, 2017.
(49) Derby, J. J.; Yeckel, A. Heat Transfer Analysis and Design for Bulk Crystal Growth: Perspectives on the Bridgman Method. In *Handbook of Crystal Growth*, Second ed.; Elsevier, 2015.
(50) Rabenau, A. The Role of Hydrothermal Synthesis in Preparative Chemistry. *Angew. Chem., Int. Ed.* **1985**, *24* (12), 1026−1040.
(51) Korzenski, M. B.; Kolis, J. W. Diels-Alder reactions using supercritical water as an aqueous solvent medium. *Tetrahedron Lett.* **1997**, *38* (32), 5611−5614.
(52) Cundy, C. S.; Cox, P. A. The Hydrothermal Synthesis of Zeolites: History and Development from the Earliest Days to the Present Time. *Chem. Rev.* **2003**, *103* (3), 663−702.
(53) Demazeau, G.; Goglio, G.; Largeteau, A. Solvothermal processes and the synthesis of nitrides. *High Press. Res.* **2008**, *28* (4), 497−502.
(54) Sun, M.; Lan, B.; Yu, L.; Ye, F.; Song, W.; He, J.; Diao, G.; Zheng, Y. Manganese oxides with different crystalline structures: Facile hydrothermal synthesis and catalytic activities. *Mater. Lett.* **2012**, *86*, 18−20.
(55) Hiley, C. I.; Lees, M. R.; Fisher, J. M.; Thompsett, D.; Agrestini, S.; Smith, R. I.; Walton, R. I. Ruthenium(V) Oxides from Low-Temperature Hydrothermal Synthesis. *Angew. Chem.* **2014**, *126*, 4512−4516.
(56) Stock, N.; Biswas, S. Synthesis of metal−organic frameworks (MOFs): routes to various MOF topologies, morphologies, and composites. *Chem. Rev.* **2012**, *112*, 933−969.
(57) Krebs, B.; Pohl, S.; Schiwy, W. Hexathio-digermanates and-distannates: A New Type of Dimeric Tetrahedral Ion. *Angew. Chem., Int. Ed.* **1970**, *9*, 897−898.
(58) Poltavets, V. V.; et al. Bulk magnetic order in a two-dimensional Ni^{1+}/Ni^{2+} (d9/d8) nickelate, isoelectronic with superconducting cuprates. *Phys. Rev. Lett.* **2010**, *104*, No. 206403.
(59) Blakely, C. K.; Bruno, S. R.; Poltavets, V. V. Low-temperature solvothermal approach to the synthesis of La4Ni3O8 by topotactic oxygen deintercalation. *Inorg. Chem.* **2011**, *50*, 6696−6700.
(60) Jana, R.; Peter, S. C. One-pot solvothermal synthesis of ordered intermetallic Pt_2In_3 as stable and efficient electrocatalyst towards direct alcohol fuel cell application. *J. Sol. St. Chem.* **2016**, *242*, 133−139.
(61) Pasco, C. M.; Trump, B. A.; Tran, T. T.; Kelly, Z. A.; Hoffmann, C.; Heinmaa, I.; Stern, R.; McQueen, T. M. Single-crystal growth of $Cu_4(OH)_6BrF$ and universal behavior in quantum spin liquid candidates synthetic barlowite and herbertsmithite. *Phys. Rev. Mater.* **2018**, *2*, No. 044406.
(62) Tran, T. T.; Quintero, M. A.; Arpino, K. E.; Kelly, Z. A.; Panella, J. R.; Wang, X.; McQueen, T. M. Chemically controlled crystal growth of $(CH_3NH_3)_2AgInBr_6$. *CrystEngComm* **2018**, *20*, 5929−5934.
(63) Tran, T. T.; Pocs, C. A.; Zhang, Y.; Winiarski, M. J.; Sun, J.; Lee, M.; McQueen, T. M. Spinon excitations in the quasi-one-

dimensional S = 1/2 chain compound $Cs_4CuSb_2Cl_{12}$. *Phys. Rev. B* **2020**, *101*, No. 235107.
(64) Wilfong, B.; Zhou, X.; Rodriguez, E. E. Hydrothermal Synthesis and Crystal Growth. In *Fundamentals of Quantum Materials: A Practical Guide to Synthesis and Exploration*; World Scientific Publishing, 2021.
(65) Feng, S.; Xu, R. New Materials in Hydrothermal Synthesis. *Acc. Chem. Res.* **2001**, *34* (3), 239−247.
(66) Scheel, H. J. Crystallization of Sulfides from Alkali Polysulfide Fluxes. *J. Cryst. Growth* **1974**, *24-25*, 669−673.
(67) Ortiz, B. R.; Gomes, L. C.; Morey, J. R.; Winiarski, M.; Bordelon, M.; Mangum, J. S.; Oswald, I. W. H.; Rodriguez-Rivera, J. A.; Neilson, J. R.; Wilson, S. D.; Ertekin, E.; McQueen, T. M.; Toberer, E. S. New kagome prototype materials: discovery of KV_3Sb_5, RbV_3Sb_5, and CsV_3Sb_5. *Phys. Rev. Mater.* **2019**, *3*, No. 094407.
(68) Berry, T.; Parkin, S. R.; McQueen, T. M. Antiferro- and metamagnetism in the S = 7/2 hollandite analog $EuGa_2Sb_2$. *Phys. Rev. Mater.* **2021**, *5*, No. 114401.
(69) Pressley, L. A.; Edey, D.; Hanna, R.; Chae, S.; Heron, J. T.; Khan, M. A.; McQueen, T. M. Informing quantum materials discovery and synthesis using X-ray micro-computed tomography. *npj Quantum Materials* **2022**, *7*, 121.
(70) Li, J.; Wang, J.; Zhang, X.; Elias, C.; Ye, G.; Evans, D.; Eda, G.; Redwing, J. M.; Cassabois, G.; Gil, B.; Valvin, P.; He, R.; Liu, B.; Edgar, J. H. Hexagonal Boron Nitride Crystal Growth from Iron, a Single Component Flux. *ACS Nano* **2021**, *15*, 7032−7039.
(71) Ribeiro, R. A.; Canfield, P. C. Solution Growth of Intermetallic Single Crystals. In *Fundamentals of Quantum Materials: A Practical Guide to Synthesis and Exploration*; World Scientific Publishing, 2021.
(72) Canfield, P. C.; Fisk, Z. Growth of single crystals from metallic fluxes. *Philosophical Magazine B* **1992**, *65* (6), 1117−1123.
(73) Jesche, A.; Canfield, P. C. Single crystal growth from light, volatile and reactive materials using lithium and calcium flux. *Philos. Mag.* **2014**, *94* (21), 2372−2402.
(74) Slade, T. J.; Canfield, P. C. Use of Refractory-Volatile Element Deep Eutectic Regions to Grow Single Crystalline Intermetallic Compounds. *Z. anorg. Allg. Chem.* **2022**, *648*, No. e202200145.
(75) Canfield, P. C.; Fisher, I. R. High-temperature solution growth of intermetallic single crystals and quasicrystals. *J. Cryst. Growth* **2001**, *225* (2−4), 155−161.
(76) Therese, G. H. A.; Dinamani, M.; Kamath, P. V. Electrochemical synthesis of perovskite oxides. *J. Appl. Electrochem.* **2005**, *35*, 459−465.
(77) Hall, C. M. Process of Reducing Aluminium from its Fluoride Salts by Electrolysis. US patent US400664, 1889.
(78) Héroult, P. French patent no. FR175711, 1886.
(79) Geiser, U.; Schlueter, J. A. Conducting organic radical cation salts with organic and organometallic anions. *Chem. Rev.* **2004**, *104*, 5203−5241.
(80) Shuku, Y.; Awaga, K. Electrochemical Synthesis and Doping for Nano-Porous Organic Magnetic Materials. *World Scientific Reference on Spin in Organics* **2018**, *4*, 207−234.
(81) Liu, Y.-H.; Yan, Y.-D.; Zhang, M.-L.; Liang, Y.; Qu, J.-M.; Li, P.; J, D.-B.; Xue, Y.; Jing, X.-Y.; Han, W. Electrochemical Synthesis of Sm-Co Metal Magnetic Materials by Co-reduction of Sm(III) and Co(II) in LiCl-KCl-$SmCl_3$-$CoCl_2$ Melt. *Elec. Acta* **2017**, *249*, 278−289.
(82) Schlueter, J. A.; Geiser, U.; Wang, H. H.; VanZile, M. L.; Fox, S. B.; Williams, J. M.; Laguna, A.; Laguna, M.; Naumann, D.; Roy, T. Electrochemical Synthesis and Crystallization of a Novel Tetraarylaurate Anion: Synthesis, Structure, and Physical Properties of (BEDT-TTF)$Au(C_6Cl_5)_4$. *Inorg. Chem.* **1997**, *36* (19), 4265−4269.
(83) Lunkenheimer, P.; Müller, J.; Krohns, S.; Schrettle, F.; Loidl, A.; Hartmann, B.; Rommel, R.; de Souza, M.; Hotta, C.; Schlueter, J. A.; Lang, M. Multiferroicity in an organic charge-transfer salt that is suggestive of electric-dipole-driven magnetism. *Nat. Mater.* **2012**, *11*, 755−758.
(84) Walsh, F. C.; Herron, M. E. Electrocrystallization and electrochemical control of crystal growth: fundamental considerations and electrodeposition of metals. *J. Phys. D: Appl. Phys.* **1991**, *24*, 217.
(85) Milchev, A. Electrochemical phase formation: some fundamental concepts. *J. Sol. St. Electrochem.* **2011**, *15*, 1401−1415.
(86) McQueen, T. M. The chemistry of quantum materials. *Comprehensive Inorganic Chemistry III, Third Edition* **2023**, 364−375.
(87) Koohpayeh, S. M.; Fort, D.; Bradshaw, A.; Abell, J. S. Thermal characterization of an optical floating zone furnace: a direct link with controllable growth parameters. *J. Cryst. Growth* **2009**, *311* (8), 2513−2518.
(88) Feigelson, R. S. Growth of fiber crystals. In *Crystal Growth of Electronic Materials*; Kaldis, E., Ed.; 1985; p 127; ISBN 978-0-444-86919-7.
(89) Stavinoha, M.; Huang, C.-L.; Phelan, W. A.; Hallas, A. M.; et al. Conductive surface states and Kondo exhaustion in insulating $YbIr_3Si_7$. *Phys. Rev. B* **2024**, *109*, No. 035112.
(90) Koohpayeh, S. M. Single crystal growth by the traveling solvent technique: A review. *Prog. Cryst. Growth Char. Mater.* **2016**, *62* (4), 22−34.
(91) Kasaya, M.; Iga, F.; Negishi, K.; Nakai, S.; Kasuya, T. A New and Typical Valence Fluctuating System, YbB_{12}. *J. Mag. Mag. Mater.* **1983**, *31−34*, 437−438.
(92) Gupta, A.; Weiser, A.; Pressley, L.; Luo, Y.; Lygouras, C.; Trowbridge, J.; Phelan, W. A.; Broholm, C. L.; McQueen, T. M.; Park, W. K. Topological surface states in the Kondo insulator YbB_{12} revealed via planar tunneling spectroscopy. *Phys. Rev. B* **2023**, *107*, No. 165132.
(93) Mason, D. R.; Cook, J. S. Zone leveling and crystal growth of peritectic compounds. *J. Appl. Phys.* **1961**, *32* (3), 475−477.
(94) Sinha, M.; Vivanco, H. K.; Wan, C.; Siegler, M. A.; Stewart, V. J.; Pogue, E. A.; Pressley, L. A.; Berry, T.; Wang, Z.; Johnson, I.; Chen, M.; Tran, T. T.; Phelan, W. A.; McQueen, T. M. Twisting of 2D Kagomé Sheets in Layered Intermetallics. *ACS Cent. Sci.* **2021**, *7* (8), 1381−1390.
(95) Hoshikawa, K. Czochralski Silicon Crystal Growth in the Vertical Magnetic Field. *Jpn. J. Appl. Phys.* **1982**, *21*, L545.
(96) Amrani, B.; Ahmed, R.; Hassan, F. E. H.; Reshak, A. H. Structural, electronic and optical properties of AgI under pressure. *Phys. Lett. A* **2008**, *372* (14), 2502−2508.
(97) Varnava, N.; Berry, T.; McQueen, T. M.; Vanderbilt, D. Engineering magnetic topological insulators in $Eu_5M_2X_6$ Zintl compounds. *Phys. Rev. B* **2022**, *105* (23), No. 235128.
(98) Berry, T.; Stewart, V. J.; Redemann, B. W. Y.; Lygouras, C.; Varnava, N.; Vanderbilt, D.; McQueen, T. M. A-type antiferromagnetic order in the Zintl-phase insulator $EuZn_2P_2$. *Phys. Rev. B* **2022**, *106*, No. 054420.
(99) Berry, T.; Varnava, N.; Ryan, D. H.; Stewart, V. J.; Rasta, R.; Heinmaa, I.; Kumar, N.; Schnelle, W.; Bhandia, R.; Pasco, C. M.; Armitage, N. P.; Stern, R.; Felser, C.; Vanderbilt, D.; McQueen, T. M. Bonding and Suppression of a Magnetic Phase Transition in $EuMn_2P_2$. *J. Am. Chem. Soc.* **2023**, *145* (8), 4527−4533.
(100) Dąbkowska, H. A.; Dąbkowski, A. B. Optical Floating Zone-Complementary Crystal Growth Technique for New Classes of Oxide Materials. In *Handbook of Crystal Growth*, 2nd ed.; 2015; pp 281−312.
(101) Hermann, R.; Priede, J.; Gerbeth, G. Floating-Zone Single Crystal Growth of Intermetallic Compounds Using a Two-phase RF Inductor. In *Handbook of Crystal Growth*, 2nd ed.; 2015; pp 313−329.
(102) Nishida, K.; Kitahama, K.; Kawai, S. Preparation of Li_3N Single Crystal By Floating Zone Technique. *J. Cryst. Growth* **1983**, *62*, 475−480.
(103) Christensen, A. N.; Rusche, C. Crystal Growth of Niobium Nitride and Niobium Carbide Nitride. *J. Cryst. Growth* **1978**, *44*, 383−386.
(104) Sakaguchi, R.; Nagao, M.; Maruyama, Y.; Watauchi, S.; Tanaka, I. Growth of Cr_2N single crystals by the floating zone method. *J. Cryst. Growth* **2020**, *546*, No. 125782.

https://doi.org/10.1021/acs.chemmater.3c03077
Chem. Mater. 2024, 36, 4929−4944

(105) Christensen, A. N. The Crystal Growth of The Transition Metal Compounds TiC, TiN, and ZrN by a Floating Zone Technique. *J. Cryst. Growth* **1976**, *33*, 99−104.
(106) Du, K.-Z.; Wang, X.; Zhang, J.; Liu, X.; Kloc, C.; Xiong, Q. CdS bulk crystal growth by optical floating zone method: strong photoluminescence upconversion and minimum trapped state emission. *Opt. Engin.* **2017**, *56* (1), No. 011109.
(107) Warren, R. W. Floating Zone Growth of Single Crystal Alkali Halides. *Rev. Sci. Instrum.* **1962**, *33*, 1378.
(108) Voronkova, V. I.; et al. Flux Growth and Properties of Oxide Crystals. In *Growth of Crystals*; Givargizov, E. I., Grinberg, S. A., Eds.; Consultants Bureau, NY, 1989; Vol. *19* (Translated by Wester, D. W.).
(109) Timofeeva, V. A. *Flux Growth of Crystals* [in Russian]; Nauka: Moscow, 1978.
(110) Elwell, D.; Scheel, H. J. *Crystal Growth from High-temperature Solutions*; Academic Press: London, 1975.
(111) Chernov, A.A.; et al.. *Modern Crystallography* [in Russian]; Nauka: Moscow, 1980; Vol. *3*.
(112) Von Dollen, P. M. *Sodium Flux Growth of Bulk Gallium Nitride*. Ph.D. Dissertation, University of California, Santa Barbara, 2016.
(113) Yamane, H.; DiSalvo, F. J. Sodium flux synthesis of nitrides. *Progr. Sol. St. Chem.* **2018**, *51*, 27−40.
(114) Parker, S. G.; Pinnell, J. E. Molten Flux Growth of Cubic Zinc Sulfide Crystals. *J. Cryst. Growth* **1968**, *3-4*, 490−495.
(115) Schleid, T.; Meyer, G. Eu_4OCl_6 and Eu_4OBr_6: Crystal Growth and Structure. *Z. anorg. allg. chem.* **1987**, *554*, 118−122.
(116) Van Loef, E. V.; Ciampi, G.; Shirwadkar, U.; Pandian, L. S.; Shah, K. S. Crystal growth and scintillation properties of Thallium-based halide scintillators. *J. Cryst. Growth* **2020**, *532*, No. 125438.
(117) Shishido, T.; Zheng, Y.; Saito, A.; Horiuchi, H.; Kudou, K.; Okada, S.; Fukuda, T. Microstructure, thermal properties and hardness of the $CeMO_3$ (M = Al, Ga) synthesized by arc-melting method. *J. Alloys. Comp.* **1997**, *260*, 88−92.
(118) Menovsky, A.; Franse, J. J. M. Crystal Growth of Some Rare Earth and Uranium Intermetallics from the Melt. *J. Cryst. Growth* **1983**, *65*, 286−292.
(119) Meier, W. R.; Du, M.-H.; Okamoto, S.; Mohanta, N.; May, A. F.; McGuire, M. A.; Bridges, C. A.; Samolyuk, G. D.; Sales, B. C. Flat bands in the CoSn-type compounds. *Phys. Rev. B* **2020**, *102*, No. 075148.
(120) Cheng, S.F.; Nadgomy, B.; Bussmann, K.; Carpenter, E.E.; Das, B.N.; Trotter, G.; Raphael, M.P.; Harris, V.G. Growth and Magnetic Properties of Single Crystal Co_2MnX (X = Si, Ge) Heusler Alloys. *IEEE Trans. Magn.* **2001**, *37* (4), 2176−2178.
(121) Johnson, D. R.; Inui, H.; Yamaguchi, M. Crystal growth of TiAl alloys. *Intermetallics* **1998**, *6*, 647−652.
(122) Oku, T. Synthesis and atomic structures of boron nitride nanotubes. *Physica B* **2002**, *323*, 357−359.
(123) Balasubramanian, C.; Godbole, V. P.; Rohatgi, V. K.; Das, A. K.; Bhoraskar, S. V. Synthesis of nanowires and nanoparticles of cubic aluminium nitride. *Nanotechnology* **2004**, *15*, 370−373.
(124) Johnston, D. C.; Moodenbaugh, A. $Zr_{3+x}S_4$: A New Superconducting Binary Sulfide. *Phys. Lett.* **1972**, *41A* (5), 447−448.
(125) Franzen, H. F.; Graham, J. Crystal structure of dihafnium sulfide*. *Z. Krist. − Cryst. Mater.* **1966**, *123*, 133−138.
(126) Hoshikawa, K.; Ohba, E.; Kobayashi, T.; Yanagisawa, J.; Miyagawa, C.; Nakamura, Y. Growth of β-Ga_2O_3 single crystals using vertical Bridgman method in ambient air. *J. Cryst. Growth* **2016**, *447*, 36−41.
(127) Schulz, D.; Ganschow, S.; Klimm, D.; Neubert, M.; Roßberg, M.; Schmidbauer, M.; Fornari, R. Bridgman-grown zinc oxide single crystals. *J. Cryst. Growth* **2006**, *296*, 27−30.
(128) May, A. F.; Yan, J.; McGuire, M. A. A practical guide for crystal growth of van der Waals layered materials. *J. Appl. Phys.* **2020**, *128*, No. 051101.
(129) Karunagaran, N.; Ramasamy, P. Synthesis, growth and physical properties of silver gallium sulfide single crystals. *Mater. Sci. Semicond. Proc.* **2016**, *41*, 54−58.
(130) Ajiboye, T. O.; Onwudiwe, D. C. Bismuth sulfide based compounds: Properties, synthesis and applications. *Res. Chem.* **2021**, *3*, No. 100151.
(131) Kucharczyk, M.; Zabludowska, K. *Review of Methods for Preparation of Zinc and Cadmium Sulfide, Selenide and Telluride Single Crystals*; 1986.
(132) Bourret-Courchesne, E. D.; Bizarri, G. A.; Borade, R.; Gundiah, G.; Samulon, E. C.; Yan, Z.; Derenzo, S. E. Crystal growth and characterization of alkali-earth halide scintillators. *J. Cryst. Growth* **2012**, *352*, 78−83.
(133) Král, R. Study on influence of growth conditions on position and shape of crystal/melt interface of alkali lead halide crystals at Bridgman growth. *J. Cryst. Growth* **2012**, *360*, 162−166.
(134) Nassau, K.; Broyer, A. M. Application of Czochralski Crystal-Pulling Technique to High-Melting Oxides. *J. Am. Ceram. Soc.z* **1962**, *45*, 474−478.
(135) Shimamura, K.; Víllora, E. G. Czochralski-based Growth and Characteristics of Selected Novel Single Crystals for Optical Applications. *Acta Phys. Polon. A* **2013**, *124* (2), 265−273.
(136) Zakgeim, D. A.; Panov, D. I.; Spiridonov, V. A.; Kremleva, A. V.; Smirnov, A. M.; Bauman, D. A.; Romanov, A. E.; Odnoblyudov, M. A.; Bougrov, V. E. Volume Gallium Oxide Crystals Grown from Melt by the Czochralski Method in an Oxygen-Containing Atmosphere. *Technol. Phys. Lett.* **2020**, *46* (11), 1144−1146.
(137) Chou, M. M. C.; Tsao, P. C.; Huang, H. C. Study on Czochralski growth and defects of $LiAlO_2$ single crystals. *J. Cryst. Growth* **2006**, *292*, 542−545.
(138) Chou, M. M. C.; Chen, C.; Yang, S. S.; Huang, C. H.; Huang, H. L. Czochralski growth and defect study of $(La,Sr)(Al,Ta)O_3$ single crystals. *J. Phys. Chem. Sol.* **2008**, *69*, 425−429.
(139) Cockayne, B.; Steward, V. W.; Brown, G. T.; MacEwan, W. R.; Young, M. L. The Czochralski Growth of Gallium Antimonide Single Crystals Under Reducing Conditions. *J. Cryst. Growth* **1982**, *58*, 267−272.
(140) Bressel, B.; Chevalier, B.; Etourneau, J.; Hagenmuller, P. Czochralski Crystal Growth of Rare Earth Tetraborides. *J. Cryst. Growth* **1979**, *47*, 429−433.
(141) Rabenau, A. Lithium Nitride and Related Materials Case Study of the Use of Modern Solid State Research Techniques. *Sol. St. Ion.* **1982**, *6*, 277−293.
(142) Walker, P. J. Melt Growth of Rare-Earth Binary and Complex Halides. *Progr. Cryst. Growth Char.* **1980**, *3* (2−3), 103−119.
(143) Lal, K.; Murthy, R. V. A.; Halder, S. K.; Singh, B. P.; Kumar, V. Growth of Nearly Perfect Alkali Halide Single Crystals by Czochralski Method and Their Characterisation. *J. Cryst. Growth* **1982**, *56*, 125−131.
(144) Olson, J. C. *A Laboratory Arc Melting Furnace for the Production of Alloy Samples from Reactive Metals*; 1961.
(145) Song, X.; Zhao, Y.; Zheng, Y. Hydrothermal synthesis of tungsten oxide nanobelts. *Mater. Lett.* **2006**, *60*, 3405−3408.
(146) Whittingham, M. S. Hydrothermal synthesis of transition metal oxides under mild conditions. *Curr. Op. Sol. St. Mater. Sci.* **1996**, *1*, 227−232.
(147) Chirayil, T.; Zavalij, P. Y.; Whittingham, M. S. Hydrothermal Synthesis of Vanadium Oxides. *Chem. Mater.* **1998**, *10*, 2629−2640.
(148) Edison, E.; Satish, R.; Ling, W. C.; Bucher, N.; Aravindan, V.; Madhavi, S. Nanostructured intermetallic $FeSn_2$-carbonaceous composites as highly stable anode for Na-ion batteries. *J. Pow. Sourc.* **2017**, *343*, 296−302.
(149) Xu, J.; Lian, Z.; Wei, B.; Li, Y.; Bondarchuk, O.; Zhang, N.; Yu, Z.; Araujo, A.; Amorim, I.; Wang, Z.; Li, B.; Liu, L. Strong Electronic Coupling between Ultrafine Iridium-Ruthenium Nanoclusters and Conductive, Acid-Stable Tellurium Nanoparticle Support for Efficient and Durable Oxygen Evolution in Acidic and Neutral Media. *ACS Catal.* **2020**, *10*, 3571−3579.

https://doi.org/10.1021/acs.chemmater.3c03077
Chem. Mater. 2024, 36, 4929−4944

(150) Jana, R.; Subbarao, U.; Peter, S. C. Ultrafast synthesis of flower-like ordered Pd_3Pb nanocrystals with superior electrocatalytic activities towards oxidation of formic acid and ethanol. *J. Pow. Sourc.* **2016**, *301*, 160−169.
(151) Xu, R.; Huang, L.; Zhang, J.; Li, D.; Liu, J.; Liu, J.; Fang, J.; Wang, M.; Tang, G. Nanostructured SnSe integrated with Se quantum dots with ultrahigh power factor and thermoelectric performance from magnetic field-assisted hydrothermal synthesis. *J. Mater. Chem. A* **2019**, *7*, 15757−15765.
(152) Huang, T.; Mao, S.; Zhou, G.; Wen, Z.; Huang, X.; Ci, S.; Chen, J. Hydrothermal synthesis of vanadium nitride and modulation of its catalytic performance for oxygen reduction reaction. *Nanoscale* **2014**, *6*, 9608−9613.
(153) Meiyan, Y.; Dong, S.; Li, K.; Hao, X.; Lai, Z.; Wang, Q.; Cui, D.; Jiang, M. Synthesis of BN nanocrystals under hydrothermal conditions. *J. Cryst. Growth* **2004**, *270*, 85−91.
(154) Kundu, J.; Khilari, S.; Pradhan, D. Shape-Dependent Photocatalytic Activity of Hydrothermally Synthesized Cadmium Sulfide Nanostructures. *ACS Appl. Mater. Interfaces* **2017**, *9*, 9669−9680.
(155) Bolagam, R.; Um, S. Hydrothermal Synthesis of Cobalt Ruthenium Sulfides as Promising Pseudocapacitor Electrode Materials. *Coatings* **2020**, *10*, 200−215.
(156) Liu, X. Hydrothermal synthesis and characterization of nickel and cobalt sulfides nanocrystallines. *Mater. Sci. Eng., B* **2005**, *119*, 19−24.
(157) Chen, Y.; Molokeev, M. S.; Atuchin, V. V.; Reshak, A. H.; Auluck, S.; Alahmed, Z. A.; Xia, Z. Synthesis, Crystal Structure, and Optical Gap of Two-Dimensional Halide Solid Solutions $CsPb_2(Cl_{1-x}Br_x)_5$. *Inorg. Chem.* **2018**, *57*, 9531−9537.
(158) Kayalvizhi, T.; Sathya, A.; Meher, K. R. S. P. Hydrothermal Synthesis of Perovskite $CsPbBr_3$: Spotlight on the Role of Stoichiometry in Phase Formation Mechanism. *J. Elec. Mater.* **2022**, *51*, 3466−3475.
(159) Wu, Q.; Liu, H.; Kang, L.; Lin, Z.; Meng, X.; Chen, X.; Qin, J. $Rb_2SeOCl_4{*}H_2O$: a polar material among the alkali metal selenite halides with a strong SHG response. *Dalton Trans.* **2016**, *45*, 17723−17728.
(160) Walton, R. I. Perovskite Oxides Prepared by Hydrothermal and Solvothermal Synthesis: A Review of Crystallisation, Chemistry, and Compositions. *Chem.—Eur. J.* **2020**, *26* (42), 9041−9069.
(161) Lai, J.; Niu, W.; Luque, R.; Xu, G. Solvothermal synthesis of metal nanocrystals and their applications. *Nano Today* **2015**, *10* (2), 240−267.
(162) Mazumder, B.; Chirico, P.; Hector, A. L. Direct Solvothermal Synthesis of Early Transition Metal Nitrides. *Inorg. Chem.* **2008**, *47* (20), 9684−9690.
(163) Choi, J.; Gillan, E. G. Solvothermal Synthesis of Nanocrystalline Copper Nitride from an Energetically Unstable Copper Azide Precursor. *Inorg. Chem.* **2005**, *44* (21), 7385−7393.
(164) Yu, S.; Yang, J.; Han, Z.; Zhou, Y.; Yang, R.; Qian, Y.; Zhang, Y. Controllable synthesis of nanocrystalline CdS with different morphologies and particle sizes by a novel solvothermal process. *J. Mater. Chem.* **1999**, *9*, 1283−1287.
(165) Hu, J. Q.; Deng, B.; Zhang, W. X.; Tang, K. B.; Qian, Y. T. Synthesis and characterization of $CdIn_2S_4$ nanorods by converting CdS nanorods via the hydrothermal route. *Inorg. Chem.* **2001**, *40* (13), 3130−3133.
(166) Chen, M.; Zou, Y.; Wu, L.; Pan, Q.; Yang, D.; Hu, H.; Tan, Y.; Zhong, Q.; Xu, Y.; Liu, H.; Sun, B.; Zhang, Q. Solvothermal Synthesis of High-Quality All-Inorganic Cesium Lead Halide Perovskite Nanocrystals: From Nanocube to Ultrathin Nanowire. *Adv. Funct. Mater.* **2017**, *27* (23), No. 1701121.
(167) Chen, L.-J.; Lee, C.-R.; Chuang, Y.-J.; Wu, Z.-H.; Chen, C. Synthesis and Optical Properties of Lead-Free Cesium Tin Halide Perovskite Quantum Rods with High-Performance Solar Cell Application. *J. Phys. Chem. Lett.* **2016**, *7* (24), 5028−5035.
(168) Imanaka, N.; Kim, Y. W.; Masui, T.; Adachi, G.-Y. Electrochemical Sc_2O_3 Single Crystal Growth. *Cryst. Growth & Design* **2003**, *3* (3), 289−290.
(169) Siegfried, M. J.; Choi, K.-S. Directing the Architecture of Cuprous Oxide Crystals during Electrochemical Growth. *Angew. Chem., Int. Ed.* **2005**, *44* (21), 3218−3223.
(170) Li, G.-R.; Zheng, F.-L.; Tong, Y.-X. Controllable Synthesis of Bi_2Te_3 Intermetallic Compounds with Hierarchical Nanostructures via Electrochemical Deposition Route. *Cryst. Growth & Design* **2008**, *8* (4), 1226−1232.
(171) Wu, H.; Maldonado, S. Electrodeposition of Pd Intermetallics using Hg-In by the Electrochemical Liquid-Liquid-Solid Method. *J. Electrochem. Soc.* **2022**, *169*, No. 112514.
(172) Toyoura, K.; Tsujimura, H.; Goto, T.; Hachiya, K.; Hagiwara, R.; Ito, Y. Optical properties of zinc nitride formed by molten salt electrochemical process. *Thin Solid Films* **2005**, *492* (1−2), 88−92.
(173) Seacrist, M. *High Quality, Low Cost Bulk Gallium Nitride Substrates Grown by the Electrochemical Solution Growth Method*; OSTI Technical Report; 2017; DOI: 10.2172/1375013.
(174) YAN, X; TAY, B; CHEN, G; YANG, S Synthesis of silicon carbide nitride nanocomposite films by a simple electrochemical method. *Electrochem. Commun.* **2006**, *8* (5), 737−740.
(175) Innocenti, M.; Becucci, L.; Bencistà; Carretti, E.; Cinotti, S.; Dei, L.; Di Benedetto, F.; Lavacchi, A.; Marinelli, F.; Salvietti, E.; Vizza, F.; Foresti, M. L. Electrochemical growth of Cu-Zn sulfides. *J. Electroanal. Chem.* **2013**, *710*, 17−21.
(176) Guan, X.; Enalls, B. C.; Clarke, D. R.; Girguis, P. Iron Sulfide Formation on Iron Substrates by Electrochemical Reaction in Anoxic Conditions. *Cryst. Growth & Design* **2017**, *17* (12), 6332−6340.

https://doi.org/10.1021/acs.chemmater.3c03077
Chem. Mater. 2024, 36, 4929−4944